

Editor's comments

Dear Editor,

The authors would like to greatly thank Theresa Blume for reviewing our revised version. To meet your request, we have revised the manuscript according to the reviewer's comments and provide our responses point by point as follows.

Best regards,

On behalf of all co-authors,

Mounir Mahdade

Anonymous Referee #1

Dear Referee,

We thank you for your insightful comments and your thorough consideration and critical review that helped us to improve our manuscript.

Kind regards,

The authors

Comment of the reviewer	Response of the authors
<i>Page 2, line 13: "any alternate morphological units": the definition of morphological units is provided later in the text (line 18), the authors might consider improving the readability of their manuscript by providing the definition in Line 13.</i>	We changed it to "to analyze any morphology characterized by alternating topographic forms (morphological units, MUs)".
<i>Page 2, paragraph 1.1: I understand the choice of using sub-paragraphs to improve the organization of the introduction, however, I found this part of the manuscript a bit abrupt. I suggest adding a sentence to clarify the consequentiality between different paragraphs.</i>	We added to the end of the paragraph: "However, it is necessary to find a method that can extract information concerning these morphologies (position, length, etc.). For this reason, it is interesting to list the works that quantitatively assess this morphological variability."
<i>Page 3, lines 19-21: could please the authors reword this sentence? Some of the terms are colloquial.</i>	I think maybe you want to write page 2 instead of page 3. We deleted "However, this may seem artificial and arbitrary".
<i>Page 4, lines 6-8: these lines repeat lines 14-15 in page 1.</i>	We deleted the repeat lines.
<i>Page 5, line 4: is "efficiency" the most appropriate term here?</i>	We changed it with "selection"
<i>Page 5, lines 6-7: the authors might consider adding a sentence or two the explain why a new method was required. I believe that such an</i>	We added a sentence to clarify: "Here, we are working with W_{bf} and with a new automatic wavelength calculation method that uses the

<i>explicit explanation would clarify the scientific relevance of this work.</i>	whole covariance structure of a set of hydraulically-independent variables, without the need of ad hoc thresholding of these variables”
<i>Page 6, line 19: why did the authors use inverted commas for the word continuous?</i>	We wanted to emphasize this property. In the final version we deleted inverted commas.
<i>Page 6, line 20: “The” should not be capitalised.</i>	Corrected
<i>Page 6, lines 21-24: albeit the authors’ strategy is reasonable, I believe that adding a few sentences to explain the reasoning underpinning the choice of the variables would increase the scientific soundness of the paper.</i>	We changed these sentences to: “This work will be done on four classical variables (velocity, hydraulic radius, bottom shear stress and local channel direction angle) because they respond directly to morphodynamic processes (flow convergence routing or meander migration) and they are independent hydraulic degrees of freedom.”
<i>Page 6, lines 28-29: I suggest explaining here the motivations that led to the choice of the BDT method as a reference (I am aware that this choice is explained later in the text, however, I feel that adding an explanation here would improve the readability of the manuscript).</i>	We changed this sentence to: “... with the bedform differencing technique (BDT) developed by O’Neill and Abrahams (1984) to determine if they yield the same results in terms of spacing. We choose this method instead of threshold methods because the latter require ad hoc thresholding / parameter range definition from independent calibration data, which was not possible in our case.”
<i>Page 8, line 5: I recommend replacing “it seems” with a sound explanation.</i>	Explanation added : “it is a more robust way of computing τ_b here than through the finite differentiation of the total head function $\frac{v(x)^2}{2g} + z(x)$ between adjacent cross-sections to get the energy slope J, given the typical number and spacing of surveyed cross-sections for each reach in the dataset.”
<i>Page 9, line 8: I think that the adjective “interesting” is too vague. The authors might consider adding one or two sentences to explain what they mean with such a qualitative word (the readers can then check the appendix to learn all the details).</i>	We changed this sentence to: “The choice of the Morlet wavelet is justified by the analytical properties in its derivation and its flexibility due to the exponential form (see Appendix B).”
<i>Page 10, line 14: “amounts” – do the authors mean “requires”?</i>	Corrected
<i>Page 10, lines 16-20: I appreciate that the authors considerably improved the structure of their first manuscript, however, these lines contains significant references that belong to the literature review.</i>	We understand this remark, however these references are related to the use of wavelets in the analysis of river morphology from a more general point of view, so we just put them as an introduction to the methodological section for the sake of brevity.
<i>Page 11, line 20: “the extraction” OF.... I suggest improving the readability of this sentence.</i>	We changed it to: “the extraction of wavelengths”

Page 12, line 6: the authors might consider adding “that is” before “the region...” to improve the readability of the sentence.	Corrected
Page 12, line 8: I suggest replacing “special” with something less colloquial. What does “special” mean in this context?	We deleted it to avoid colloquial terms.
Page 12, line 11: is the reference to equation 8 correct?	Yes, it is the definition of the phase: $\phi(x, s) = \text{Im}(\ln W[f(x)](x, s))$ So we can replace it in the equation: $\frac{\partial}{\partial x} \text{Im}(\ln W[f(x)](x, s)) - k = 0$
Page 12, line 24: please remove “the” before “Eq.14”.	Corrected
Page 15, lines 7-8: I suggest rewording this sentence to match the writing style of a scientific publication.	We changed it to: “But then the local wavenumber would be specific to a given variable. Otherwise, the multivariate case requires to determine a common wavenumber between all the variables such that:”
Page 15, lines 18-20: could please the authors clarify this sentence?	We changed it to: “The procedure is applied to a set of variables $[v, R_h, \tau_b, \theta]$ and the goal is to seek for the common wavenumber between all these variables. In the Fig. 7, we illustrate the result of this procedure applied on the Olivet River for all the four variables. A unique wavenumber is extracted which represents a co-evolution of all these variables. As a result, the phase shift of every variable is calculated by:”
Page 16, line 10: could please the authors clarify the meaning of “which is corrected afterwards.”?	We mean that this shift is corrected in the following positions. So, we changed it to: “is corrected in the following x positions”
Page 18, line 8: could please the authors reword “work onto an...”?	We changed it to: “The wavelet method extracts the wavelength for an assessed length ...”
Page 19, lines 7-22: in my opinion, the readers can infer these pieces of information (by themselves) from the table. Could please the authors provide an in-depth interpretation of these results?	We added a comment at the end of the section : “However, there is no direct way of validating the estimates from these raw results : a way of doing so would be to build a synthetic, equivalent periodic geometry parameterized by the identified wavelength in order to verify that it yields, for example, a similar reach-average rating curve. This will be the subject of further work.”
Page 19, line 24: could please the authors explain the choice of the word “interestingly”? How “interestingly”?	We changed it to “Consequently”. It is the interpretation of what has been said before.
Page 21, line 6: the BDT method has already been introduced. I suggest avoiding this repetition.	We deleted the repetition.
Page 21, line 7: the BDT method does not require expert judgement, however, is the BDT method	We added: “... the literature (i.e., BDT). This method shows good results in the identification of

<i>accurate? Could please the authors provide some reference?</i>	these bedforms according to some researches (e.g., Frothingham and Brown, 2002; Krueger and Frothingham, 2007).
<i>Page 22, line 14: could please the authors explain and reword “is done a sort of multiple calculations”?</i>	We changed this to: “while BDT does not directly calculate the wavelength. It is computed by averaging the pool-to-pool and riffle-to-riffle distances.”
<i>Page 22, line 21: could please the authors replace “reasonable” with a quantitative or semi-quantitative assessment? In my opinion, “reasonable” is too vague.</i>	We replaced it with: “This indicates that a length greater than two cycles (pool-riffle) is always required ...”
<i>Page 22, line 25: could please the authors elaborate on the potential reasons underpinning this “big difference”?</i>	We added some reasons: “This difference is due to the choice of the tolerance value, which is low in our case to the point of not filtering out the high-frequency variability of bed elevation and therefore gives a lower periodicity compared to the wavelets.”
<i>Page 24, lines 2-3: what is the difference between “benchmark” and “reference” in this context?</i>	Benchmark means an example from the literature and a reference method is a true and accurate method. For that we will delete “reference” to avoid the misunderstanding.
<i>Page 25, line 17: the authors might consider adding a reference to the paragraph presenting the “good results” or a quantitative assessment.</i>	We added a comment on performance : “Ultimately, hydraulic modeling will be the true test of the potential of a pseudo-periodic equivalent geometry (e.g. for simulating a reach-average rating curve)”
<i>Page 25, line 26: I believe that the authors meant to write “it presents”.</i>	Corrected
<i>Page 25, line 28: please rephrase “we can say the same thing”.</i>	We replaced it with: “Similarly”.
<i>Page 26, line 7: please reword “on the overall”.</i>	We replaced it with: “As a result”.

References:

Frothingham, K. M., & Brown, N. (2002). Objective identification of pools and riffles in a human-modified stream system. *Middle States Geographer*, 35, 52-60.

Krueger, A. and Frothingham, K.: Application and comparison of geomorphological and hydrological pool and riffle quantification methods, *Geogr Bull*, 48, 85–95, 2007.

O'Neill, M. P., & Abrahams, A. D. (1984). Objective identification of pools and riffles. *Water resources research*, 20(7), 921-926.

Referee #2: Gregory Pasternack, gpast@ucdavis.edu

Dear Gregory Pasternack,

We thank you for your insightful comments and your thorough consideration and critical review that helped us to improve our manuscript.

Your initial review was very constructive that's why we gave our best to make this work much better.

Kind regards,

The authors

(1) In the methods section, there is a lengthy explanation of the equations, but only a very brief phrase mentioning how all of the work was actually implemented. I think it is important to help enable readers who want to follow in the authors' footsteps to be able to repeat the work with their own data. I checked the website provided as well as the link to Scilab. The information the authors provided is not enough. Please clarify if there already exists a program, module, package, etc that adapts the wavelet code for use in Scilab or if that was something you made yourself? if it already exists, clarify if it may be obtained via the Scilab website or if one has to go elsewhere to get it. if you adapted it yourself, then you should provide a link to that code in the article, preferably to a free, open hosting website like Github. I see that the wavelet analysis tools have been moved to Github and of course Scilab is free, open. Therefore, you should enable readers to follow your lead and use your tools rather than have to reinvent them on their own. This is simple to address.

Response:

First, the use of Scilab is quite similar to Matlab. So we download the toolbox of Torrence and Compo (1998) [atoc.colorado.edu/research/wavelets/] in Matlab version and we have made some easy syntax changes. This toolbox is also available in Python. Second, the main thing that we have done is solving of

the equation $\frac{\partial \phi}{\partial x} - k = 0$ which is easy to make. For that, we simplify the computing of term $\frac{\partial \phi}{\partial x}$ based on

well-known functions like $\mathcal{W}[f(x)](x, k)$, $\mathcal{W}[xf(x)](x, k)$, ... (this was detailed in the Appendix B).

(2) there are several spelling and grammar mistakes that can be refined through careful scrutiny of the text. This time I am not going to provide that type of editing, because I think the authors should address that.

Response:

We corrected all spelling and grammar mistakes.

(3) In the discussion section, I would like to see the authors add a paragraph that would "close the loop" applying the results to the introduction's motivation issue, which was design of hydraulic models. Do you envision wavelet tools being used to design river morphology for use in hydraulic models based on your work? if so, what are your thoughts on how that would be done? River Builder 1.0.0 was recently released on Github, now in Python, at <https://github.com/RiverBuilder/RiverBuilder>. It does not have wavelet as of yet, but it could if that is something the authors recommend.

Response:

We added this paragraph in line 24-25:

“This wavelength can be used to represent the variability of the bathymetry in hydraulic models in cases where we do not have access to the bottom of the channel (e.g., remote sensing data as the overcoming Surface Water and Ocean Topography Mission) and the morphology can be modelled by pseudo-periodic functions. Furthermore, it can be implemented in synthetic geometry generators (e.g., River Builder, Pasternack and Zhang, 2020) where the bathymetry and sinuosity wavelengths extracted by the wavelets can be used to model meandering rivers with alternating morphologies. Ultimately, hydraulic modeling will be the true test of the potential of a pseudo-periodic equivalent geometry (e.g. for simulating a reach-average rating curve).”

References:

Pasternack, G.B. and Zhang, M. 2020. River Builder User’s Manual For Version 1.0.0. University of California, Davis, CA. <https://github.com/RiverBuilder/RiverBuilder>

Torrence, C. and Compo, G. P.: A practical guide to wavelet analysis, Bulletin of the American Meteorological society, 79, 61–78, 1998.

Automatic identification of alternating morphological units in river channel using wavelet analysis and ridge extraction

Mounir Mahdade¹, Nicolas Le Moine¹, Roger Moussa², Oldrich Navratil³, and Pierre Ribstein¹

¹Sorbonne Université, CNRS, EPHE, Milieux environnementaux, transferts et interaction dans les hydrosystèmes et les sols, METIS, F-75005 Paris, France

²INRA, UMR LISAH, 2 Place Pierre Viala, 34060 Montpellier, France

³University of Lyon, Lumière Lyon 2, Department of Geography, CNRS 5600 EVS, France

Abstract The accuracy of hydraulic models depends on the quality of the bathymetric data they are based on, whatever the scale at which they are applied. The along-stream (longitudinal) and cross-sectional geometry of *natural* rivers is known to vary at the scale of the hydrographic network (e.g., generally decreasing slope, increasing width), allowing parameterizations of main cross-sectional parameters with large-scale proxy such as drainage area or bankfull discharge (an approach coined downstream hydraulic geometry, DHG). However, higher-frequency morphological variability (*i.e.*, at river reach scale) is known to occur for many stream types, associated with varying flow conditions along a given reach, as for instance, the alternate bars or the pool-riffle sequences and meanders. To consider this high-frequency variability of the geometry in the hydraulic models, a first step is to design robust methods to characterize the scales at which it occurs. In this paper, we introduce new wavelet analysis tools in the field of geomorphic analysis (namely, Wavelet Ridge Extraction), in order to identify the pseudo-periodicity of alternating morphological units from a general point of view (focusing on pool-riffle sequences) for six small French rivers. This analysis can be performed on a single variable (univariate case) but also on a set of multiple variables (multivariate case). In this study we chose a set of four variables describing the flow degrees of freedom: velocity, hydraulic radius, bed shear stress, and a planform descriptor which quantifies the local deviation of the channel from its mean direction. Finally, this method is compared with the Bedform Differencing Technique (BDT), by computing the mean, median, and standard deviation of their longitudinal spacings. The two methods show agreement in the estimation of the wavelength in all reaches except one. The aim of the method is to extract a pseudo-periodicity of the alternating bedforms that allow objectively identifying morphological units in a continuous approach with the respect of correlations between variables (*i.e.*, At Many Station Hydraulic Geometry, AMHG) without the need to define a prior threshold for each variable to characterize the transition from one unit to another.

1 – Introduction:

Hydraulic modeling is based on the description of river morphology (cross-sectional geometry), and this is their essential input despite its scarcity and cost of acquisition. In fact, the most important aspect to know is the river bathymetric data at the local scale, detailed and specific to the site and local conditions (Alfieri et al., 2016). This component is important for an accurate modeling of river hydraulics such as flood modeling (e.g., Neal et al., 2015; Trigg et al., 2009), river restoration (e.g., Wheaton et al., 2004a), ecohydraulics (e.g., Pasternack and Brown, 2013), environmental modeling and fluvial process (e.g., Rodriguez et al., 2013).

Many researchers are working on determining the best simplified representation of channel geometry (Saleh et al., 2013; Grimaldi et al., 2018), based on the variability of cross sections but without the knowledge of the bed elevation variability or the river sinuosity at smaller scale. Other studies focused on the generating of river channels with taking into account the sub-reach scale variability using geostatistics and variogram tools (Legleiter, 2014a, 2014b) or a geometric framework modeling with geomorphic covariance structures

(Brown et al., 2014). Longitudinal variability in river geometry may have greater impact on the simulation of the water level than the cross-sectional shapes (Saleh et al., 2013) and it must be taken into account in the hydraulic models. This topographic variability is related to the channel morphology types. In this study, we focus mainly on alternating alluvial channels especially pool-riffle sequences, even though the method presented here could be used to analyze any alternate morphology characterized by alternating topographic forms (morphological units, μ MUs). The objective is to provide a continuous description of geometric and flow patterns along a reach, a description that could be subsequently used to create a synthetic river as in the RiverBuilder (Brown et al., 2014). To do that we calculate the dimensionless reach wavelength λ^* , which is the distance between pools (or riffles) divided by average channel width (e.g., Richards, 1976a; Keller and Melhorn, 1978; Carling and Orr, 2000) or bankfull width (e.g., Leopold et al., 1964). However, it is necessary to find a method that can extract information concerning these morphologies (position, length, etc.). For this reason, it is interesting to list the works that quantitatively assess this morphological variability.

1 – 1 – State of art methods for a quantitative assessment of morphological variability within a reach:

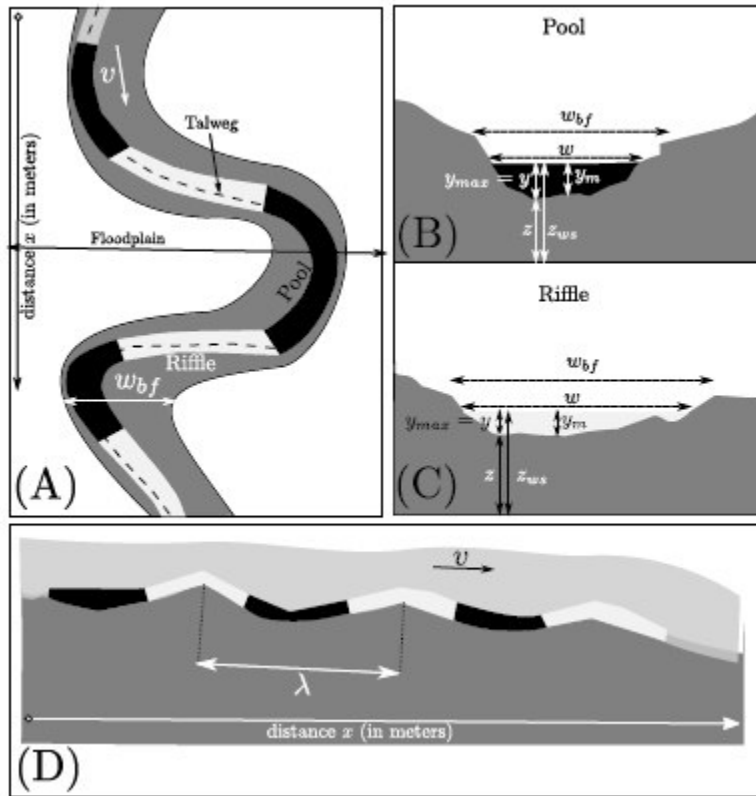
Morphological units are topographic forms that shape the river corridor (Wadeson, 1994; Wyrick et al., 2014). They form alternating and rhythmic undulations continuously varying along the river (Thompson, 2001). This continuity is difficult to represent, for this reason most of the methods that model these patterns divide the topography into discrete units to analyze them. ~~However, this may seem artificial and arbitrary~~ (Kondolf, 1995; Wyrick et al., 2014).

Among the most frequently observed alternating MUs, pools and riffles have been recognized as fundamental geomorphological elements of meandering streams (Krueger and Frothingham, 2007). In fact, pools are located in the outer edge of each meander loop and defined as topographic lows along a longitudinal stream profile with high depth and low velocity (Fig. 1 (A), (B) and (D)) and research has shown that they generally have an asymmetrical cross section shape. Conversely, riffles are topographic highs with shallow depths and moderate to high velocities located in the straight parts of the reach between adjacent loops (Fig. 1 (A), (C) and (D)) and have symmetrical cross section shapes (O'Neill and Abrahams, 1984; Knighton, 1981).

For many years, many researchers have been trying to develop techniques to identify MUs and especially pools and riffles using hydraulic variables or topographic ones, or both (table 1). In the one dimensional identification, some studies used bed topography only to determine the characteristics of MUs. Richards (1976a) proposed the zero-crossing method which fits a regression line to the longitudinal profile of the bed elevation and defines pools as points that have negative residuals and riffles as points with positive residuals. O'Neill and Abrahams (1984) developed the Bedform Differencing Technique (BDT) as a refinement of Richards' methodology. This one uses bed elevations measured at a fixed interval along the channel to calculate the bed elevation difference series between local extrema (maximum and minimum) of the bed profile. The BDT introduces a tolerance value (T), which is the minimum absolute value of the cumulative elevation change required for the identification of a pool or riffle. The value of T is based on the standard deviation (S_D) of the bed elevation difference series and eliminates the erroneous classification of small undulations in the bed profile. Another method proposed by Knighton (1981) as the Areal Difference Asymmetry Index which is defined as the ratio of the difference between the area of the right and the left of channel centerline on the total cross-sectional area to identify the location of pools and riffles by their symmetrical or asymmetrical areas. On the other hand, some studies focused only on hydraulic parameters to identify MUs. For example, Yang (1971) proposed an identification of pools and riffles using the energy gradient and affirmed that the fundamental difference between riffles and pools is the difference in energy

1 gradients. Also, Jowett (1993) proposed a classification criterion with Froude number and velocity/depth
 2 ratio to distinguish between pools, runs, and riffles.

3



4

5 **Figure 1.** Different views of pool-riffle sequences. (A) Plan view pattern that includes bankfull width w_{bf} , floodplain
 6 extent, talweg line, velocity v , pools and riffles, and channel direction (planform); (B) cross-sectional view of a pool
 7 with a section width w and a steeper water depth y calculated from the talweg elevation, which is the deepest part of
 8 the bottom, and $y = y_{max} = z_{ws} - z$ with z is the bed elevation and z_{ws} the water surface elevation, and y_m the
 9 mean water depth; (C) cross-sectional view of a riffle with a shallower water depth y , higher bed elevation z and high
 10 bankfull width w_{bf} ; (D) longitudinal profile that makes it possible to see the water surface, the bed slope, the pools
 11 and riffles, and the wavelength λ calculated between two successive riffles or pools

12 All these methods handle topographic or hydraulic parameters separately. Recently, however, several
 13 researchers have improved MUs identification through the use of the covariance of several parameters in a
 14 multidimensional approach. Schweizer et al. (2007) used a joint depth and velocity distribution to predict
 15 pools, runs, and riffles without the knowledge of the river bathymetry. Hauer et al. (2009) used a functional
 16 linkage between depth-averaged velocity, water depth and bottom shear stress to describe and quantify six
 17 different hydro-morphological units (riffle, fast run, run, pool, backwater and shallow water) using a
 18 conceptual Mesohabitat Evaluation Model (MEM) under various flow conditions. These methods use digital
 19 elevation models (DEMs) to extract more information about MUs. In this purpose, Milne and Sear (1997)
 20 began with depth to define pool-riffle sequences using ArcGis tools and DEMs to model the geometry of
 21 river channels based on field surveyed cross-sections on a three-dimensional basis. But, by choosing depth
 22 alone, the difference between two bedforms with the same depth becomes difficult to know. In contrary, it
 23 is easy with different bed slopes and bed roughness that yield different velocities and shear stresses (Wyrick

1 et al., 2014). So to overcome this and take into account the lateral variation of rivers, Wyrick et al. (2014)
2 proposed a new method for the objective identification and mapping of landforms at the morphological unit
3 scale. They used spatial grids of depth and velocity at low flow estimated using 2D hydrodynamic model
4 and an expert classification scheme that determine the number and the nomenclature of MUs and range of
5 base flow depth and velocity of each type.

6 Brown and Pasternack (2017) chose two variables: the minimum bed elevation and the channel top width
7 across several flow discharges. They calculated the geomorphic covariance structure (GCS) which is a
8 bivariate spatial relationship amongst or between standardized and possibly detrended variables along a
9 river corridor. They found that there is a positive correlation between these two variables. Also, they used
10 an autocorrelation function and power spectral density to prove a quasi-periodic pattern of wide and shallow
11 or narrow and deep cross sections along the river. This pioneer work and other studies (e.g., Richards, 1976;
12 Carling and Orr, 2002) proved that a single longitudinal cycle may contain a pool with a narrow and deep
13 cross section, a riffle with a wide and shallow cross section, in addition to transitional forms. The work that
14 we present in this paper aim to present a spectral method that extract this pseudo-periodicity from a river in
15 order to characterize the alternating MUs and especially pool-riffle sequences, and to identify the key
16 parameter (the wavelength) that characterizes the scale of variability of the river topography. This
17 information can be further used to build a synthetic river such as the RiverBuilder (Pasternack and
18 ~~Arroyo~~Zhang, 20182020) or the channel builder for simulating river morphology of Legleiter (2014).

19 Some of the methods presented in the literature have shown limits in calculating the wavelengths of pool-
20 riffle sequences, others have given results that are often difficult to interpret in terms of bedform amplitude.
21 This amplitude, which varies according to each bedform, involves the use of the pseudo-period. In fact, few
22 methods are developed to extract this pseudo-period from alternating MUs rivers. We therefore choose to
23 work with wavelet analysis that estimates the local variability strength of a signal and extract the signal
24 amplitude and wavelength. In this study we apply continuous wavelet transform (CWT) to calculate the
25 wavelength λ and the dimensionless wavelength spacing λ^* (longitudinal spacing) which is ~~a normalization~~
26 ~~of λ by the reach average bankfull width (w_{bf})~~.

$$\lambda^* = \frac{\lambda}{w_{bf}} \quad (1)$$

27 With w_{bf} is bankfull width.

Methods	Variables	MUs	References
Control-point method	Energy gradient	Pools and riffles	Yang (1971)
Zero-crossing method	Bed topography	Pools and riffles	Richards (1976a) ; Milne (1982)
Areal difference asymmetry index	Cross-section area	Pools and riffles	Knighton (1981)
Power spectral analysis	Bed topography	Pools and riffles	Nordin (1971) ; Box and Jenkins (1976)
Bedform Differencing Technique (BDT)	Bed topography	Pools and riffles	O'Neill and Abrahams (1984)
Hydraulic characteristics classification	Froude number	Pools, runs, and riffles	Jowett (1993)
3D identification	Water depth	Pools and riffles	Milne and Sear (1997)
Schweizer's method	Water depth and velocities	Pools, runs, and riffles	Schweizer et al., 2007a
MEM Model	Water depth, velocity, and bottom shear stress	Pool, riffle, run, fast run, shallow water, and backwater	Hauer et al (2009), Hauer et al (2011)
Wyrick's method	Water depth and velocity	Pools, riffles, runs, and glides	Wyrick et al. (2014), Wyrick and Pasternack (2014)
Brown and Pasternack method	Minimum bed elevation and channel top width	Pools and riffles	Brown and Pasternack (2017)

1 **Table 1:** Review of some methods of morphological units' identification (variable used and MUs types).

2 In reality, longitudinal spacing λ^* has several definitions. Some authors have defined the wavelength λ as
3 the distance between riffle crests (e.g., Harvey (1975); Hogan et al. (1986)), or the distance from the bottom
4 of successive pools (e.g., Keller and Melhorn (1973, 1978)). Other authors have chosen channel width w
5 (e.g., Richards (1976a, b); Dury (1983)) instead of bankfull channel width w_{bf} (e.g., Leopold et al. (1964)).
6 These differences raise questions about the efficiencyselection of these ratios and their dependence on
7 geometric or hydraulic parameters. Moreover, the majority of researchers uses the average channel width
8 instead of the bankfull width because both give a similar pool-riffle spacing interval. Here, we are working
9 with w_{bf} and with a new automatic wavelength calculation method ~~that we present in section 3~~ that uses
10 the whole covariance structure of a set of hydraulically-independent variables without the need of ad hoc
11 thresholding of these variables.

12 Some researchers have investigated the variability of longitudinal spacing in relation to geometric or
13 hydraulic parameters. Rosgen (2001) developed an empirical relationship between the ratio of pool-to-pool
14 spacing/bankfull width and the channel slope expressed as a percentage based on a negative power function
15 of slope S :

$$\lambda^* = 8.2513 \times S^{-0.9799} \quad (2)$$

16
17 In addition, Montgomery et al. (1995) showed that there is an influence of large woody debris (LWD) on
18 channel morphology that leads to a relation between LWD and longitudinal spacing in a pool-riffle
19 sequence, and found that 82% of pools were formed by LWD or other obstructions, and increased numbers
20 of obstructions led to a decrease in pool-riffle spacing. Moreover, research has linked variation in spacing
21 to channel characteristics including gradient (Gregory et al., 1994). Also, Harvey (1975) showed that pool-
22 riffle spacing correlated strongly with discharges between the mean-annual flood and a 5 year recurrence
23 interval (Thompson, 2001). Recently, Wyrick and Pasternack (2014) measured spacing of six different
24 morphological units using a tool in ArcGIS. Therefore, the definition of the characteristics and the

1 measurement methods allowed us to expect some variation from one study to another in the estimated
2 relationship between longitudinal spacing and bankfull width (Richards, 1976a; O'Neill and Abrahams,
3 1984; Gregory et al., 1994; Knighton, 1998). Aside from the interval $[5w_{bf}, 7w_{bf}]$ defined by Leopold et
4 al. (1964) and the interval $[2w_{bf}, 4w_{bf}]$ defined by Montgomery et al. (1995) in forested streams, other
5 values of the spacing longitudinal exist, such as the Carling and Orr (2000) interval, which is $[3w_{bf}, 7.5w_{bf}]$
6 and decreases to $[3w_{bf}, 6w_{bf}]$ as sinuosity increases (Clifford, 1993; Carling and Orr, 2000).

7 **1 – 2 – Study objectives:**

8 The studies that used wavelet analysis in the geomorphological field consist in extracting components of a
9 given spatial series (e.g., $w(x)$, $v(x)$), but they are not specifically designed to identify pseudo-periodic
10 components in a univariate, let alone in a multivariate case. For this reason, we introduce an automatic
11 procedure called Wavelet Ridge Extraction defined by Lilly and Olhede (2009) and used in this study to
12 extract the longitudinal spacing of the alternating MUs.

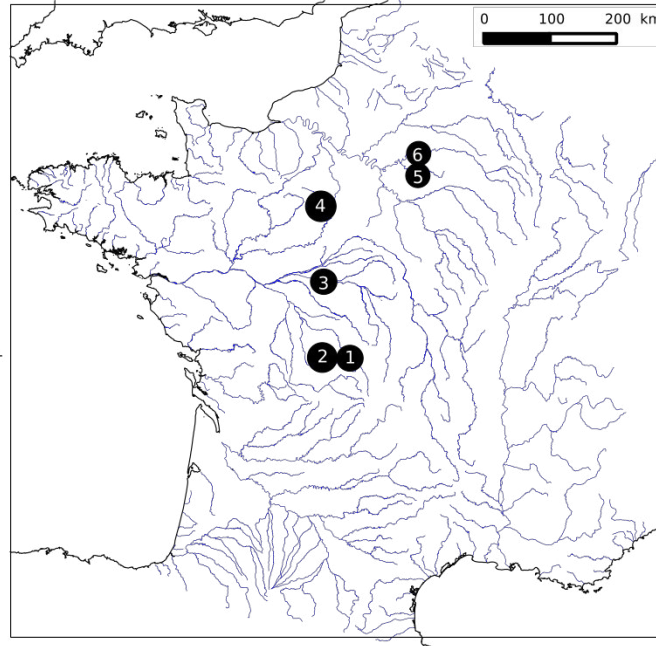
13 The objective is to extract some quantitative properties of these alternating morphological units such as the
14 mean and the median of their longitudinal spacing, with a “continuous” vision of the topography instead of
15 a discrete classification. This will be done by focusing on two numerical criteria computed at reach scale:
16 ~~The distribution of spacings between morphological units (mean, median, etc.) and the evaluation of~~
17 ~~correlations between all geometrical and flow variables. This work will be done on four classical variables~~
18 ~~such as (velocity, hydraulic radius, and bottom shear stress, with the addition of a variable less used in the~~
19 ~~identification of pools and riffles namely, and the local channel direction angle). because they respond~~
20 ~~directly to morphodynamic processes (flow convergence routing or meander migration) and they are~~
21 ~~independent hydraulic degrees of freedom. This variable will be used to evaluate the impact of the river~~
22 ~~sinuosity in the determination of wavelengths and also in the localization of MUs.~~

23 In this study, we first present the dataset of six river reaches in France used for this analysis (section 2). In
24 section 3, we present the Wavelet Ridge Extraction method to identify pool-riffle sequences in the univariate
25 and multivariate cases with ~~the four variables (velocity, hydraulic radius, bottom shear stress, and local~~
26 ~~channel direction angle). Section 4 presents results and compare them with the bedform differencing~~
27 ~~technique (BDT) developed by O'Neill and Abrahams (1984) to determine if they yield the same results in~~
28 ~~terms of spacing. We choose this method instead of threshold methods because the latter require ad hoc~~
29 ~~thresholding / parameter range definition from independent calibration data, which was not possible in our~~
30 ~~case. To accomplish this, we calculate the wavelength λ and the longitudinal spacing λ^* .~~

31 **2 - Data set and study reaches:**

32 Six reaches of small French rivers are used in this study (Navratil, 2005; Navratil et al., 2006): the Graulade
33 at St Sylvain Montaignut (1), the Semme at Droux (2), the Olivet at Beaumont Village (3), the Ozanne at
34 Tirzay lès Bonneval (4), the Avennelles at Boissy-le-Châtel Les Avennelles (5), and the Orgeval at Boissy-
35 le-Châtel Le Theil (6) (Fig. 2). These reaches contain mainly pool-riffle sequences, they have slopes
36 between 0.002 and 0.013 m.m⁻¹ (estimated from the talweg elevation which is the lowest point in the
37 section), mobile gravel beds, stable banks, and well-defined floodplains along at least one side of the channel
38 (Navratil et al., 2006). These reaches are located in the Loire River Basin (four reaches) and the Seine River
39 Basin (two reaches), and their length ranges from 155 to 495 m (Table 2). All reaches are located at or near
40 the stream gauging stations of the French national hydrometric network. Long-term (about 20 years)
41 hydrological records are available for most reaches. The bankfull widths vary from 4 to 12 m, with an
42 average value of about 9 m.

The Loire river basin
 (1) the Graulade in St
 Sylvain Montaigut
 (2) the Semme in Droux
 (3) the Olivet in
 Beaumont Village
 (4) the Ozanne in
 Tirzay lès Bonneval
 The Seine river basin
 (5) the Avennelles in Boissy-
 le-Châtel Les Avennelles
 (6) the Orgeval in Boissy-
 le-Châtel Le Theil



1

2 **Figure 2.** Location of the study reaches in France.

3 Cross-sections were surveyed along the river reaches at the level of hydraulic controls and morphological
 4 breaks in order to describe the major variations in terms of width, height, and slope in the main channel and
 5 the floodplain and at the level of pool-riffle sequences. Cross-sections and water surface profile
 6 measurements were surveyed in 2002 – 2004 covering the main channel and floodplain and using an
 7 electronic, digital, total-station theodolite. Water surface profiles were measured at different flow discharges
 8 (Navratil et al., 2006).

Reach	1: Graulade	2: Semme	3: Olivet	4: Ozanne	5: Avennelles	6: Orgeval
Reach length L (m)	160	177	495	319	155	318
Number of cross sections	14	32	66	26	25	36
Reach gradient S (m.m ⁻¹)	0.0125	0.0044	0.0018	0.0024	0.0060	0.0047
Bankfull width w_{bf} (m)	4	12	6	12	9	10
Average width w_m (m)	2.8	9.3	4.7	7.0	3.3	6.1
Standard deviation $\sigma(w)$ (m)	0.4	1.9	0.9	1.1	0.9	1.0
Surveyed flow discharges (m ³ .s ⁻¹)	0.22 and 1.26	1.85 and 2.41	0.18, 1.13, 1.72, and 1.99	0.19, 0.33, 0.8, and 11.5	0.15	0.21
Min discharge Q_{min} (m ³ .s ⁻¹)	0.22	1.85	0.18	0.19	0.15	0.21

9 **Table 2.** Characteristics of the six river reaches and their catchment. The bankfull width w_{bf} is taken from the study
 10 of Navratil et al. (2006), and the average width w_m , the standard deviation $\sigma(w)$ are calculated for the minimum
 11 discharge used in this study Q_{min} .

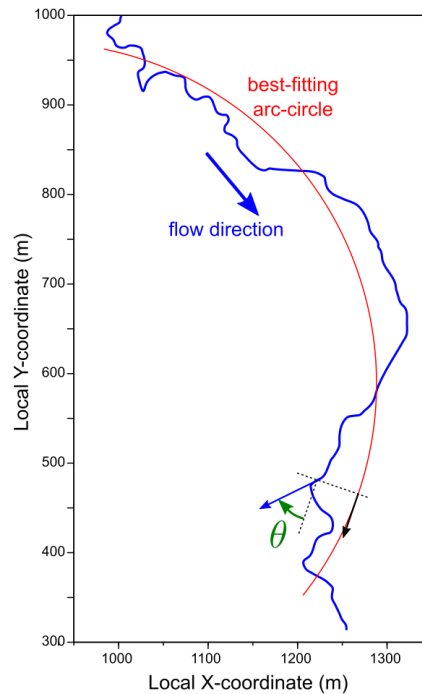
12 Using this dataset, we solely rely on measurements at the lowest surveyed discharge in the development of
 13 the method because it is the discharge through which we can visualize the variability of the bathymetry
 14 (alternating morphological units). We select four spatial series:

15 1) velocity $v(x)$;

- 1 2) hydraulic radius $R_h(x) = \frac{A(x)}{P(x)} \cong \frac{A(x)}{w(x)}$ with $A(x)$ is the cross-section area and $P(x)$ is the wetted
- 2 perimeter;
- 3 3) **b**Bed shear stress $\tau_b(x) = (\rho g)n^2v(x)^2R_h(x)^{-1/3}$ with ρ : water density ($1000 \text{ kg}\cdot\text{m}^{-3}$) and n is
- 4 the Manning's roughness coefficient;
- 5 4) **L**ocal channel direction angle (planform) $\theta(x)$.

6 All descriptors are derived from in-situ observations taken from Navratil et al. (2006), except the calibrated
7 estimates of Manning's roughness coefficient n . These values were estimated by Navratil et al. (2006) using
8 a one-dimensional open channel steady and step backwater model FLUVIA (Baume and Poirson, 1984).
9 However, we will use these in order to compute the bed shear stress $\tau_b(x)$, along the reach: even if partly
10 relies on calibration, it ~~is seems~~ a more robust way of computing τ_b here than through the finite
11 differentiation of the total head function $\frac{v(x)^2}{2g} + z(x)$ between adjacent cross-sections to get the energy
12 slope J , given the typical number and spacing of surveyed cross-sections for each reach in the dataset.

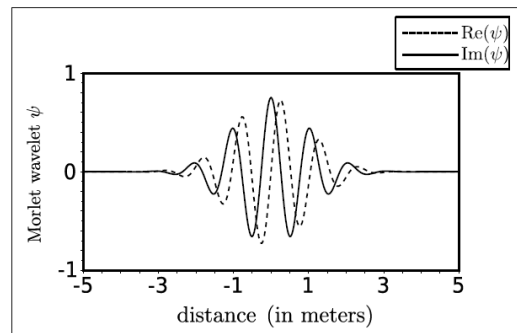
13 The fourth variable chosen is related to the channel planform: we define $\theta(x)$ as the local angular deviation
14 of the channel direction from a lower-frequency curve. There are many possible definitions of this low-
15 frequency behavior, such as parametric splines or Bezier curves; in order to avoid over-parameterization,
16 we define this low-frequency planform as a constant curvature curve, i.e., the best-fitting arc-circle (Fig. 3),
17 a choice suitable for all six reaches studied. Since θ is signed, it is expected to have a pseudo-periodicity
18 which is approximately twice slower as other 1D variables: indeed, a large positive value of θ indicates a
19 counterclockwise deviation from the low-frequency direction, while a large negative value of same
20 amplitude indicates a clockwise deviation. From a hydraulic perspective, both deviations have the same
21 effect since they are symmetrical with respect to the low-frequency direction. For this reason, which chose
22 to analyze the variable $\cos(\theta(x))$.



1 **Figure 3.** Definition of θ , the local angular deviation of the channel direction from a lower-frequency behavior. Here
2 this low-frequency planform is defined as an arc-circle (illustration on the Olivet River reach). It is worth noting that
3 θ is signed: at the location pointed on the figure, θ is negative.

4 **3 – Wavelet method**

5 Classical mathematical methods, such as Fourier analysis, extract the wavelengths in the frequency domain
6 for stationary signals, but can also be used for nonstationary signals using an “evolutive” methodology based
7 on spectral estimators (Thomson., 1982; Pasternack and Hinnov., 2003). Wavelet transform standardly does
8 the same for nonstationary signals: analyzing a signal basically consists in looking for local similarity
9 between the signal and a given waveform (the wavelet). In this paper, we use the continuous wavelet
10 transform with the Morlet wavelet (Gabor, 1946) (Fig. 4) applied to spatial series instead of time series, so
11 periods and frequencies in time series are replaced by wavelengths (in m) and wavenumbers (in rad.m^{-1}).
12 The choice of the Morlet wavelet is justified by the analytical properties in its derivation and its flexibility
13 due to the exponential form ~~its interesting analytical properties~~ (see Appendix B).



14
15 **Figure 4.** Morlet mother wavelet function. The plot gives the real part and the imaginary part of the wavelets in the
16 space domain (distance).

17 The wavelet transform uses a whole family of “daughter” wavelets generated by scaling and translating the
18 mother wavelet ψ ; the value of the transform at location x and scale s is the scalar product of the signal and
19 this daughter wavelet $\psi_{s,x}$.

20 Wavelet analysis is very popular in many fields such as fluid mechanics (e.g., Schneider and Vasilyev
21 (2010); Higuchi et al. (1994); Katul et al. (1994); Katul and Parlange (1995b, a)), meteorology (e.g., Kumar
22 and Foufoula-Georgiou (1993); Kumar (1996)), geophysics (e.g., Ng and Chan (2012); Grinsted et al.
23 (2004)), hydrology (e.g., Rossi et al. (2011); Schaeffli et al. (2007); Nourani et al. (2014)), and
24 geomorphology (Lashermes et al., 2007; Gangodagamage et al., 2007; McKean et al., 2009). In the literature
25 of the alternating bedforms identification, McKean et al. (2009) used Derivative of a Gaussian wavelets
26 (DOG) of order 6 to investigate the spatial patterns (pools and riffles) of channel morphology and salmon
27 spawning using a one-dimensional elevation profile of the channel bed morphology.

28 In this study, we use another application of the wavelet analysis called the wavelet ridge extraction method
29 (Mallat, 1999; Lilly and Olhede, 2010). This analysis is based on the existence of special space/wavenumber
30 curves, called wavelet ridge curves or simply ridges (Lilly and Olhede, 2010), where the signal concentrates
31 most of its energy (Carmona et al., 1999; Ozkurt and Savaci, 2005). Along such a curve, the signal can be
32 approximated by a single component modulated both in amplitude and frequency. So, the rationale behind
33 the method is that the existence of alternating morphological units along a reach (such as pools-riffles
34 sequences) could be translated into a pseudo-periodicity in geometric and flow variables. Hence, identifying

1 these bedforms requires amounts to identifying a local wavenumber $K(x)$ and phase $\Phi(x)$ for each variable,
 2 a task that can be performed by wavelet analysis and especially Wavelet Ridge Extraction (Mallat, 1999;
 3 Lilly and Olhede, 2010).

4 5 **3 – 1 – Wavelet analysis and ridge extraction:**

6 Few methods in the literature have been trying to identify river characteristics with wavelets. For example,
 7 Gangodagamage et al. (2007) used Wavelet Transform Modulus Maxima (WTMM, Muzy et al., 1993) in a
 8 fractal analysis to extract multiscale statistical properties of a corridor width. Procedures such as the WTMM
 9 consist in extracting components of the signal, but they are not specifically designed to identify pseudo-
 10 periodic components in a univariate, let alone in a multivariate case.

11 In the present study, we tested a new wavelet ridge analysis on spatial series with the Morlet mother basis
 12 function represented in Fig. 4. Its expression is:

$$\psi(\eta) = \pi^{-\frac{1}{4}} e^{i\beta\eta} e^{-\frac{\eta^2}{2}} \quad (3)$$

13 With ψ is the mother wavelet function that depends on the dimensionless "position" parameter η and β is
 14 the dimensionless frequency, here taken to be 6 as recommended by Torrence and Compo (1998). Starting
 15 with this wavelet mother, a family $\psi_{s,x}$ called wavelet daughters is obtained by translating and scaling ψ .

$$\psi_{s,x}(\eta) = \frac{1}{\sqrt{s}} \psi\left(\frac{\eta - x}{s}\right), x \in \mathbb{R}, s > 0 \quad (4)$$

16 With x is the translation offset, which represents a position at which the signal is analyzed, and s the dilation
 17 or scale factor.

18 If $s > 1$, the daughter wavelet has a frequency lower than the mother wavelet, whereas if $s < 1$, a wavelet
 19 with a frequency higher than the mother wavelet is generated.

20 Given a spatial series $f(\eta)$, its continuous wavelet transform $W[f](x, s)$ with respect to the wavelet ψ is a
 21 function of two variables where:

$$W[f]: \mathbb{R} \times \mathbb{R}_+^* \rightarrow \mathbb{C} \\ (x, s) \rightarrow \frac{1}{\sqrt{s}} \int_{-\infty}^{+\infty} f(\eta) \psi^*\left(\frac{\eta - x}{s}\right) d\eta \quad (5)$$

22 (*) indicates the complex conjugate. This complex function can also be written as:

$$W[f](x, s) = R(x, s) e^{i\phi(x, s)} \quad (6)$$

23 With R is the absolute value (modulus) and ϕ the phase (argument) at position x with the scale s .

$$R(x, s) = |W[f](x, s)| \quad (7)$$

$$\phi(x, s) = \text{Im}(\ln W[f(x)](x, s)) \quad (8)$$

24 To respect the nomenclature in the spatial definition and facilitate the extraction, extraction of wavelengths,
 25 we choose the angular wavenumber (in rad.m^{-1}) $k = \frac{2\pi}{\lambda}$ instead of the scale factor. We associate a
 26 wavelength $\lambda = 2\pi\alpha s$ with the scale parameter s , where α is the Fourier factor associated with the wavelet,
 27 and

$$\alpha = \frac{2}{\beta + \sqrt{2 + \beta^2}} \quad (9)$$

$$s = \frac{1}{\alpha k} \quad (10)$$

1 Thus, the wavelet transform of the function $f(x)$ is defined in the space-wavenumber as:

$$W[f]: \mathbb{R} \times \mathbb{R}_+^* \rightarrow \mathbb{C} \\ (x, s) \rightarrow \sqrt{\alpha k} \int_{-\infty}^{+\infty} f(\eta) \psi^*(\alpha k(\eta - x)) d\eta \quad (11)$$

2 Except for the channel angle, all input variables are always positive and may substantially vary in magnitude
3 so we perform the wavelet transform on the Neperian logarithm of these variables. The whole analysis is
4 performed in [a simple Scilab script](#), using ~~an adaptation~~ [the functions that compute the wavelet transform](#)
5 [W\[f\]. They were provided —of the toolbox—](#) by Torrence and Compo (1998)
6 [atoc.colorado.edu/research/wavelets/]. [To extract the wavelength, the procedure in Appendix B is](#)
7 [followed to compute \$\frac{\partial \phi}{\partial x}\$ and extract the curves that satisfy Eq. 12 and 13.](#)

8 The complex wavelet transform can be classically visualized using a scalogram, i.e., a colored map of the
9 modulus $R(x, k)$ in the (x, k) plane (Fig. 5 bottom). The wavelet analysis neglects parts of the signal at both
10 extremities of the series: this is the *cone of influence* (Torrence and Compo., 1998); [that is](#) the region of the
11 wavelet spectrum in which edge effects become important. However, as explained previously, the complex
12 transform also yields a phase ~~$\phi(x, k)$~~ $\Phi(x, k)$ in rad (Eq. (8)) which can also be plotted in the same plane
13 (Fig. 5 top). In our study, we will search for ~~special~~ space/wavenumber curves mainly using the phase
14 information, i.e. search for *phase ridges* as opposed to *amplitude ridges* (Lilly and Olhede, 2010).

15 In section 3.2, we give a rigorous definition of Wavelet Ridge points and curves in a univariate case (i.e., a
16 single spatial series). Then, in section 3.3, we generalize the definition to the multivariate i.e. when the
17 series consists in several correlated variables.

18 3 – 2 – Univariate case:

19 In the univariate case, we choose a single variable f (velocity, hydraulic radius, bed shear stress, or local
20 channel direction angle). For the wavelet $\psi(\eta)$, the ridge point of $W[f](x, k)$ is a space/wavenumber pair
21 (x, k) satisfying the *phase ridge point conditions* (Lilly and Olhede, 2010):

$$\frac{\partial}{\partial x} \text{Im}(\ln W[f(x)](x, k)) - k = 0 \quad (12)$$

22

23 or, according to the definition of the phase (Eq. 8) :

$$\left. \frac{\partial \phi}{\partial x} \right|_{(x, k)} - k = 0 \quad (13)$$

24

25 This condition states that the rate of change of transform phase at scale k exactly matches k at location x ;
26 from this condition, the instantaneous frequency of the signal can be derived (Lilly and Olhede, 2008 ;
27 Lilly and Olhede, 2010). The sets of points satisfying the condition form a parametric curve (ridge curve)
28 noted $(x, K(x))$ ~~implicitly~~ [implicitly](#) defined by:

$$\left. \frac{\partial \phi}{\partial x} \right|_{(x, K(x))} - K(x) = 0 \quad (14)$$

1 This property is illustrated in Fig. 5, where a ridge curve is superposed both on the scalogram and on the
 2 phase map.

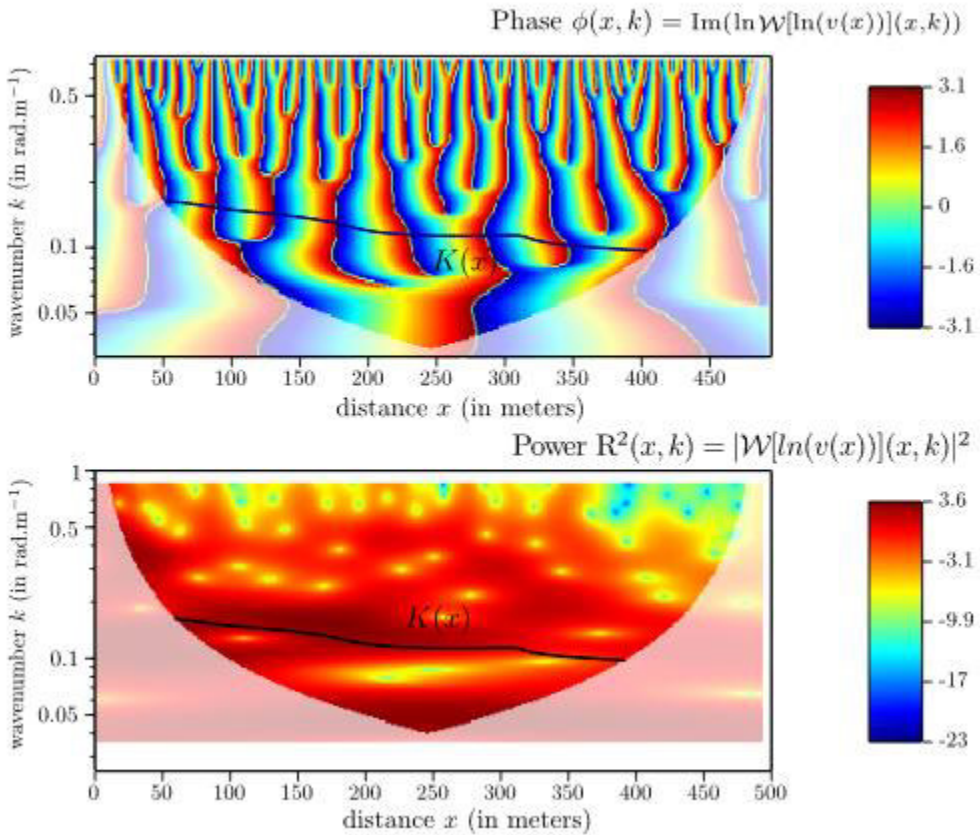
3 There may be several curves that verify the Eq. 14; in practice we choose curves that cross continuously the
 4 domain of the wavelet transform (from one cone of influence to another) and belong to the region where a
 5 maximum power of the wavelet is. This curve $K(x)$ also represents the local wavenumber, which is defined
 6 on a support $\ell < L$ named assessed length, with L the total reach length.

7 The phase function Φ is then obtained by evaluating the function $\phi(x, k)$ along the curve $(x, K(x))$, in thick
 8 black in Fig. B1 (A) in Appendix B-1.

$$\Phi(x) = \phi(x, K(x)) \quad (15)$$

9 In the end, we can extract the wavelength function of pool-riffle sequences, which corresponds to a pseudo-
 10 period function of the signal f , and which is:

$$\lambda(x) = \frac{2\pi}{K(x)} \quad (16)$$



11
 12 **Figure 5:** Top plot: the phase function from which we get the function $K(x)$; bottom plot: the power of the wavelet
 13 with the region where there is maximum variability depicted by the black curve $K(x)$ (ridge curve). These two
 14 figures are represented in a wavenumber/distance space for the Olivet River and the wavelet transform is performed
 15 on the logarithm of the velocity. The part of the figure with low opacity shows the cone of influence which is
 16 neglected in this study (edge effects are more important for short wavelengths than for long wavelengths).

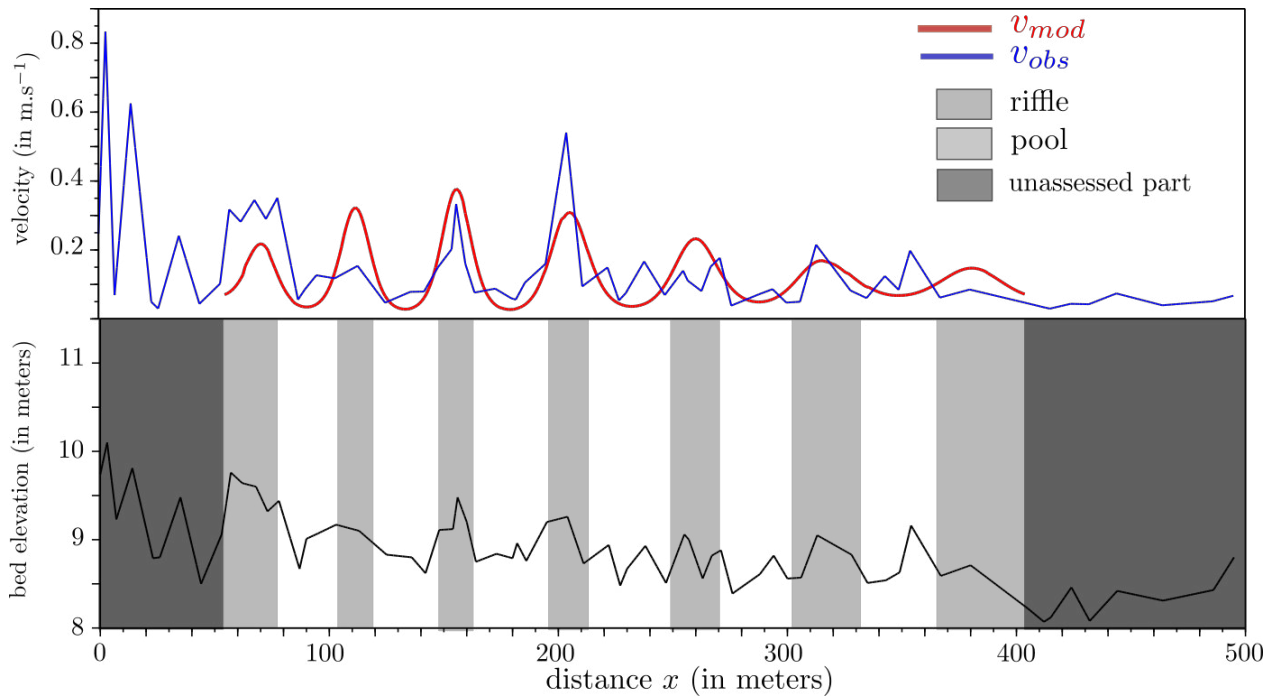
1 Also, the shape's amplitude A_m , with which pools and riffles vary, is corrected by a coefficient $\sqrt{\frac{1}{\alpha K(x)}}$. This
 2 correction comes from the inversion of the direct transformation equation (Eq. 11) which holds the
 3 coefficient $\sqrt{\alpha K(x)}$.

$$A_m(x) = |W[f](x, K(x))| \sqrt{\frac{1}{\alpha K(x)}} = R(x, K(x)) \sqrt{\frac{1}{\alpha K(x)}} \quad (17)$$

4 The signal is locally similar to a sinusoid f_{mod} of wavenumber K in rad.m^{-1} which model the variability f .
 5 We can define the pseudo-periodic variable as presented in the Fig. 6 with:

$$f_{mod}(x) = A_m(x) \cos(\Phi(x)) = A_m(x) \cos(\phi(x, K(x))) \quad (18)$$

6 In the example below (Fig. 6), the modeled velocity function follows the variability of the observed velocity,
 7 it is a pseudo-periodic, continuous function that approximates the first-order variability of this hydraulic
 8 parameter across pool-riffle sequences. The statistics of the $K(x)$ function can be translated into statistics of
 9 longitudinal spacings of alternating bedforms, e.g. mean spacing λ^*_{mean} , median spacing λ^*_{median} or
 10 spacing standard deviation $\sigma(\lambda^*)$. In Fig. 6 we would find $\lambda^*_{mean} \approx 8.7$, $\lambda^*_{median} \approx 9.12$, and $\sigma(\lambda^*) \approx$
 11 0.79 if we were to analyze velocity only ; The pseudo-periodicity of v_{mod} yields to the identification of 6
 12 pools (white) and 7 riffles (gray).



13
 14 **Figure 6:** variation of the modeled function f_{mod} which represent the pseudo-periodic variable (e.g., the velocity of
 15 the Olivet River) compared to the observed one. This pseudo-periodicity yields to the identification of pools (white)
 16 and riffles (gray) in the plot below. The not studied part is due to the cone of influence of the wavelet method.

17
 18

1 In the next section, we will extend the definition of phase ridge points and ridges to the case where several
 2 variables are sampled along the reach, all of them potentially correlated and embedding information about
 3 the pseudo-periodicity of channel hydraulic behavior.

4 3 – 3 – Multivariate case:

5 The multivariate case is the extension of the univariate to a set of N real-valued signals, we use the
 6 coevolution of more than one variable to extract the wavelength of the reach and therefore identify the pool-
 7 riffle sequences. We start by computing the wavelet transform for each variable $i = 1..N$ and extract their
 8 phase functions $\phi_i(x, k)$. According to the previous section, univariate ridges curves $K_i(x)$ would be defined
 9 by:

$$\frac{\partial \phi_i}{\partial x} \Big|_{(x, K_i(x))} - K_i(x) = 0 \quad (19)$$

10

11 But then the local wavenumber would be specific to a given variable, Otherwise, the multivariate case
 12 requires to determine a common wavenumber between all the variables which is not what we would like.
 13 We would rather like to find a common wavenumber for all variables at location x, i.e. such that:

$$\frac{\partial \phi_i}{\partial x} \Big|_{(x, K(x))} - K(x) \approx 0 \quad \forall i \quad (20)$$

14

15 The identification of a “master” ridge point/curve is now a minimization problem. We will define it as a
 16 local minimum of the squared norm of the vector $\left(\frac{\partial \phi_1}{\partial x} \Big|_{(x, k)} - k, \frac{\partial \phi_2}{\partial x} \Big|_{(x, k)} - k, \dots, \frac{\partial \phi_N}{\partial x} \Big|_{(x, k)} - k \right)$:

$$E(x, k) = \sum_{i=1}^N \left(\frac{\partial \phi_i}{\partial x} \Big|_{(x, k)} - k \right)^2 \quad (21)$$

17 This minimum is calculated by searching for the wavenumbers and positions where the derivatives (Equ.
 18 22) of this quantity satisfies these two conditions bellow:

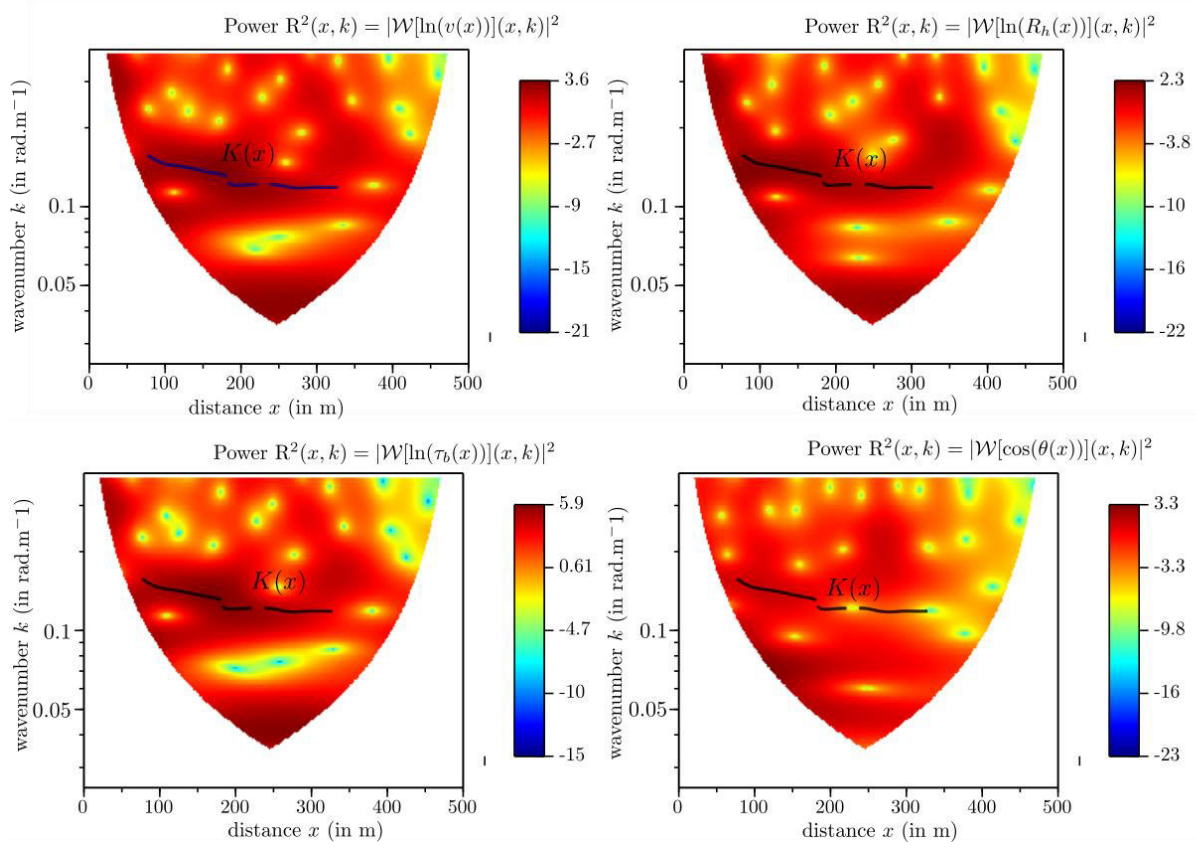
$$\begin{aligned} \frac{\partial E(x, k)}{\partial k} &= \sum_{i=1}^N \left(\frac{\partial^2 \phi_i}{\partial k \partial x} \Big|_{(x, k)} - 1 \right) \left(\frac{\partial \phi_i}{\partial x} \Big|_{(x, k)} - k \right) = 0 \\ \frac{\partial^2 E(x, k)}{\partial k^2} &= \sum_{i=1}^N \left[\frac{\partial^3 \phi_i}{\partial k^2 \partial x} \Big|_{(x, k)} \left(\frac{\partial \phi_i}{\partial x} \Big|_{(x, k)} - k \right) + \left(\frac{\partial^2 \phi_i}{\partial k \partial x} \Big|_{(x, k)} - 1 \right)^2 \right] > 0 \end{aligned} \quad (22)$$

19 The procedure is applied to a set of variables. An illustration of this procedure is given in Fig. 7 for the Olivet
 20 River. As mentioned in section 2 the set of variables is $[v, R_h, \tau_b, \theta]$. The power of the wavelet changes
 21 according to the variables but the pseudo-period is common to all four variables, which represents a co-
 22 evolution of these variables; and the goal is to seek for the common wavenumber between all these variables.
 23 In the Fig. 7, we illustrate the result of this procedure applied on the Olivet River for all the four variables.
 24 A unique wavenumber is extracted which represents a co-evolution of all these variables.

25 And by the same procedure as in the univariate case As a result, the phase shift of every variable is calculated
 26 by:

$$\Phi_i(x) = \phi_i(x, K(x)) \quad (23)$$

- 1 This ridge curve $K(x)$ is common between all variables, yet Φ_i varies according to each variable. Therefore,
 2 each one can be represented as a pseudo-periodic function $f_{i,mod}$ with the pair $(K(x), \Phi_i(x))$.

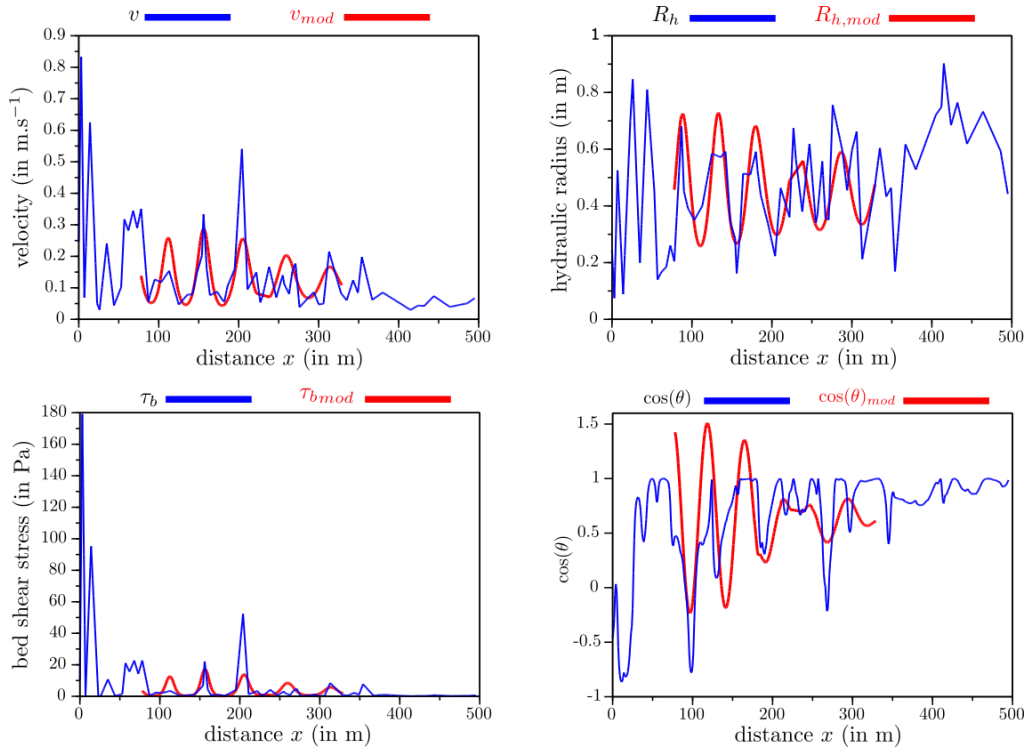


- 3
 4 **Figure 7:** Power of the wavelet of the four variables: velocity, hydraulic radius, bed shear stress, and local channel
 5 direction angle. The black curve $K(x)$ is the extracted ridge curve of the Olivet River in the multivariate case.
 6 In our case, after calculating the phase and amplitude, we modelled each variable as in the Eq. 24 and
 7 represented them in Fig. 8.

$$f_{i,mod}(x) = A_{i,m}(x) \cos(\Phi_i(x)) = A_{i,m}(x) \cos(\phi_i(x, K(x))) \quad (24)$$

- 8
 9 The amplitude shape of the modeled variable is calculated by the same way in the univariate case:

$$A_{i,m}(x) = |\mathcal{W}[f_i](x, K(x))| \sqrt{\frac{1}{\alpha K(x)}} \quad (25)$$



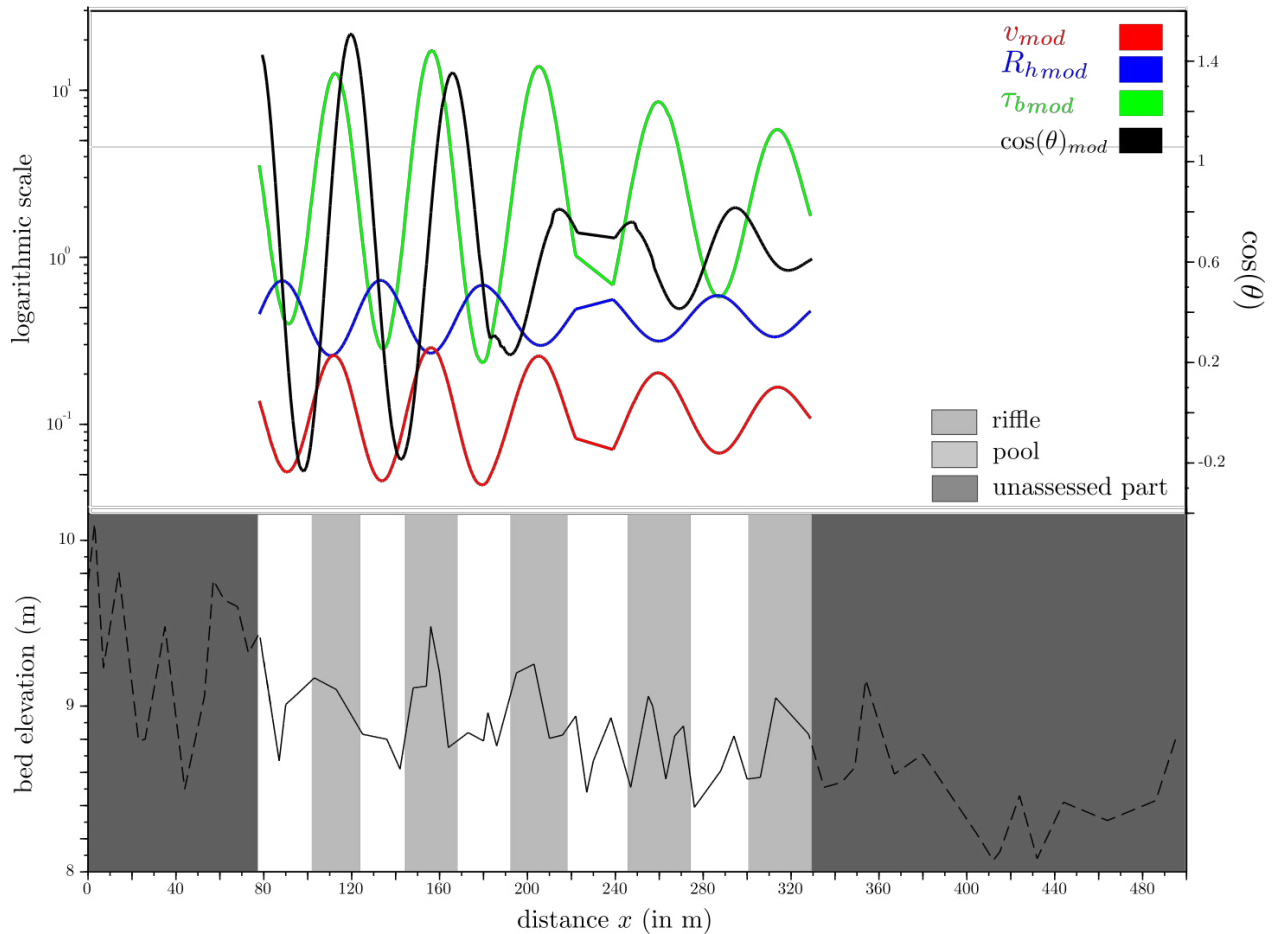
1
2 **Figure 8:** Variation of the modeled function $f_{i,mod}$ which represent the pseudo-periodic variable (in red) for the
3 velocity, the hydraulic radius, the bed shear stress, and the local channel direction angle of the Olivet River compared
4 to the observed ones (in blue).

5 The results in Fig. 8 show that a common pseudo-period has been successfully ~~identified~~ and
6 allows a consistent pseudo-periodic representation of all four variables.

7 Fig. 9 shows the correlations between these variables which are well respected between the three flow
8 variables; an anti-correlated hydraulic radius with bed shear stress and velocity and a strong correlation
9 between bed shear stress and velocity. However, with regard to the angle, the results show a small phase
10 shift which is corrected in the following x positions afterwards. But generally a deviation (clockwise or
11 counterclockwise) from the average direction of the channel (i.e. $\cos(\theta)$ much smaller than 1) is associated
12 with a low hydraulic radius and large values of τ_b and v , a consistent characterization of a riffle. This gives
13 us an identification reach features: pools (in white) and riffles (in grey).

14 As already mentioned in section 3.2 (univariate analysis), the statistics of the $K(x)$ function can be translated
15 into statistics of local wavelength $\lambda(x) = 2\pi/K(x)$, which can in turn be interpreted as statistics of
16 longitudinal spacings of alternating bedforms, e.g. mean spacing λ^*_{mean} , median spacing λ^*_{median} or
17 spacing standard deviation $\sigma(\lambda^*)$. In the example of the Olivet river (Fig. 9) $\lambda^*_{mean} \approx 8.16$, $\lambda^*_{median} \approx$
18 8.62 , and $\sigma(\lambda^*) \approx 0.70$. The pseudo-periodicity of the set $[v_{mod}, R_{h,mod}, \tau_{b,mod}, \theta_{mod}]$ yields to the
19 identification of 5 pools and 5 riffles.

20 ~~And then, a continuous topography can be generated that models the observed one using the local~~
21 ~~wavenumber $K(x)$. The validation of this approach will be undertaken in the next section by comparing~~
22 ~~these univariate and multivariate approaches by modelling the topography and validating with the measured~~
23 ~~one to determine how well our approach holds.~~



1
 2 **Figure 9:** Correlation between the modeled functions $f_{i,mod}$ which represent the pseudo-periodic variables (velocity
 3 in red, hydraulic radius in blue, bed shear stress in green, and local channel direction angle in black) of the Olivet river.

4 – Results:

5 In this section, we present the results of the analysis on the six reaches presented in section 2. We present
 6 the comparison between the univariate and the multivariate approaches and a comparison of the multivariate
 7 with the benchmark method. The methods are compared in terms of the statistics (mean, median, etc.) they
 8 yield. Second, we present the benchmark method called BDT (Bedform differencing technique) and
 9 compare ~~its~~their results of the six reaches with the multivariate case.

10 4 – 1 – Univariate vs Multivariate:

11 First, both approaches were employed on all reaches to extract statistics such as the mean, median and
 12 standard deviation wavelengths of morphological units (pool-riffle sequences). The wavelet method extracts
 13 the wavelength for an ~~works onto an~~ assessed length ℓ (which is the $K(x)$ support in Fig. 6 and 9) that is
 14 generally small compared to the total length of the reach. Consequently, we have results that are valuable
 15 only for the lengths shown in Table 3. In this table, we give the values of these lengths for each approach
 16 and with the variables used in it. These values generally depend on the number of alternating bed forms and
 17 also on the total length of the reach. The greater the number of alternating bed forms and the reach length
 18 are, the greater the assessed length is.

1 Moreover, the multivariate approach takes into account all the variables and therefore looks for a single
 2 pseudo-periodicity between the four variables and then we're going to have a pseudo-periodicity that
 3 represents the reach and not the chosen variable.

Reaches	Reach length (m)	Assessed length ℓ (m) (Univariate)				Assessed length ℓ (m) (Multivariate)
		Velocity	Hydraulic radius	Bed shear stress	Local channel direction angle	$[v, R_h, \tau_b, \cos\theta]$
1: Graulade	160	88	67	72	102	67
2: Semme	177	87	70	89	110	37
3: Olivet	495	349	366	363	365	251
4: Ozanne	319	215	157	151	125	77
5: Avenelles	155	76	70	79	64	60
6: Orgeval	318	142	200	163	140	158

4 **Table 3.** Assessed length by the wavelet analysis for all reaches in the univariate case using the velocity, hydraulic
 5 radius, bed shear stress, or local channel direction angle and in the multivariate case using all these four variables.

6 Table 4 gives some statistics on both approaches. Longitudinal spacing is calculated using the wavelengths
 7 extracted automatically by the wavelet ridge method from $K(x)$.

8 We compare the methods in terms of longitudinal spacing (λ^*). In each reach, there seems to be one variable
 9 which drives the wavelength identified in the multivariate approach:

- 10 - in the Graulade River, the longitudinal spacing identified using the multivariate approach matches
 11 closely the one associated with the hydraulic radius (in the mean and the median with deviation of
 12 $0.05w_{bf}$) and also with the local channel direction angle (in the median with a deviation of
 13 $0.06w_{bf}$);
- 14 - in the Semme River, it matches those of the local channel direction angle (in the mean and the
 15 median with a deviation of $0.14w_{bf}$ and $0.12w_{bf}$ consecutively);
- 16 - in the Olivet River, it matches the bed shear stress (in the mean with a deviation of $0.25w_{bf}$) and
 17 the velocity (in the median with a deviation of $0.5w_{bf}$);
- 18 - in the Ozanne River, it matches those of the hydraulic radius and the velocity (in the mean and the
 19 median with a deviation less than $0.6w_{bf}$);
- 20 - in the Avenelles, it matches those of the velocity, hydraulic radius, and the bed shear stress (in the
 21 mean with a deviation less than $0.15w_{bf}$);
- 22 - in the Orgeval River, it matches those of the hydraulic radius (in the mean with a deviation of
 23 $0.28w_{bf}$ and the median with $0.06w_{bf}$) and also with the local channel direction angle (in the mean
 24 with a deviation of $0.23w_{bf}$ and in the median with $0.11w_{bf}$).

				1: Graulade	2: Semme	3: Olivet	4: Ozanne	5: Avennelles	6: Orgeval
Univariate	Velocity	$\lambda(m)$	Mean	23.47	13.86	52.20	37.18	27.32	51.66
			median	24.17	13.93	54.74	36.74	27.17	51.29
			$\sigma(\lambda)$	1.69	0.53	7.75	2.97	1.60	1.70
		λ^*	Mean	5.87	1.15	8.70	3.10	3.03	5.17
			median	6.04	1.16	9.12	3.06	3.02	5.13
			$\sigma(\lambda^*)$	0.42	0.04	1.29	0.25	0.18	0.17
	Hydraulic radius	$\lambda(m)$	Mean	21.74	39.28	47.19	37.73	25.72	45.46
			median	21.41	39.43	46.60	38.47	25.47	48.23
			$\sigma(\lambda)$	0.71	1.19	4.74	2.40	0.66	8.73
		λ^*	Mean	5.43	3.27	7.86	3.14	2.86	4.55
			median	5.35	3.29	7.76	3.20	2.83	4.82
			$\sigma(\lambda^*)$	0.18	0.10	0.79	0.20	0.07	0.87
Bed shear stress	$\lambda(m)$	Mean	26.07	32.29	47.47	36.43	27.47	51.70	
		median	25.92	32.66	45.54	36.30	27.95	51.26	
		$\sigma(\lambda)$	1.12	1.68	5.36	1.70	0.73	1.54	
	λ^*	Mean	6.52	2.69	7.91	3.04	3.05	5.17	
		median	6.48	2.72	7.59	3.02	3.11	5.13	
		$\sigma(\lambda^*)$	0.28	0.14	0.89	0.14	0.09	0.15	
$\cos\theta$	$\lambda(m)$	Mean	21.14	23.45	40.87	66.31	28.79	50.58	
		median	21.32	23.30	39.44	62.98	28.73	49.93	
		$\sigma(\lambda)$	0.75	0.95	3.57	7.49	1.47	4.35	
	λ^*	Mean	5.28	1.95	6.81	5.52	3.20	5.06	
		median	5.33	1.94	6.57	5.25	3.19	4.99	
		$\sigma(\lambda^*)$	0.19	0.08	0.60	0.62	0.16	0.43	
Multivariate	$[v, R_h, \tau_b, \cos\theta]$	$\lambda(m)$	Mean	21.54	21.74	48.98	43.89	26.59	48.29
			median	21.55	21.84	51.70	43.49	26.54	48.78
			$\sigma(\lambda)$	0.38	0.85	4.22	0.98	0.40	3.42
		λ^*	Mean	5.38	1.81	8.16	3.66	2.95	4.83
			median	5.39	1.82	8.62	3.62	2.95	4.88
			$\sigma(\lambda^*)$	0.09	0.07	0.70	0.08	0.04	0.34

1 **Table 4.** Summary of results for all reaches in the univariate case using the velocity, hydraulic radius, bed shear stress,
2 or local channel direction angle and in the multivariate case using all these four variables. For each variable we compute
3 the mean, median, and the standard deviation σ of the wavelength and the longitudinal spacing. This one λ^* is
4 calculated by $\frac{\lambda}{w_{bf}}$, and w_{bf} is taken from Table 2.

5 Interestingly Consequently, the multivariate estimates of λ^* compares with univariate estimates in a similar
6 way:

- 7 - The distribution of λ^* in the multivariate case is included in the envelope of univariate distributions,
- 8 - The dispersion of this multivariate distribution, measured by $\sigma(\lambda^*)$, is always close to the minimum
9 value that can be achieved by any of the univariate distributions.

10 Hence, the multivariate method improves the identification of the wavelength: it is less sensitive to a local
11 high frequency variation of a given variable if this variation is not associated with a variation of the others
12 variables. However, there is no direct way of validating the estimates from these raw results : a way of doing
13 so would be to build a synthetic, equivalent periodic geometry parameterized by the identified wavelength
14 in order to verify that it yields, for example, a similar reach-average rating curve. This will be the subject of
15 further work.

16 In the following section, we will compare the wavelet method with a benchmark method using talweg
17 elevation.

1 4 – 2 – Comparison with benchmark method:

2 In this section, we compare our method's results with a selected benchmark method from the literature (i.e.
3 BDT). This method shows good results in the identification of these bedforms according to some researches
4 (e.g., Frothingham and Brown, 2002; Krueger and Frothingham, 2007). ~~It is called the Bed form~~
5 ~~Differencing Technique (BDT) introduced by O'Neill and Abrahams (1984). We choose this method instead~~
6 ~~of threshold methods because the latter require thresholds (expert judgment) collected from the field, which~~
7 ~~is not possible in our case.~~

8 The technique of O'Neill and Abrahams (1984) (BDT) uses a tolerance value (T), which defines the
9 minimum absolute value needed to identify a pool or a riffle (Krueger and Frothingham, 2007). It is
10 calculated using the standard deviation (S_D) of the series of bed elevation differences from upstream to
11 downstream for each reach and corrected by a coefficient chosen according to the reach. For this, we test
12 several tolerance values, and for the Graulade (1), Ozanne (4), Avennelles (5) and Orgeval (6) reaches we
13 find the same results. We choose to check one tolerance value for each reach with $T = S_D$. This method
14 gives pools and riffles positions by assigning a crest as a riffle and a bottom as a pool and therefore the
15 computation of the wavelengths becomes a little difficult. So, we chose to calculate a series of pool-pool
16 and riffle-riffle spacings, their medians, and standard deviations and then calculate their averages.

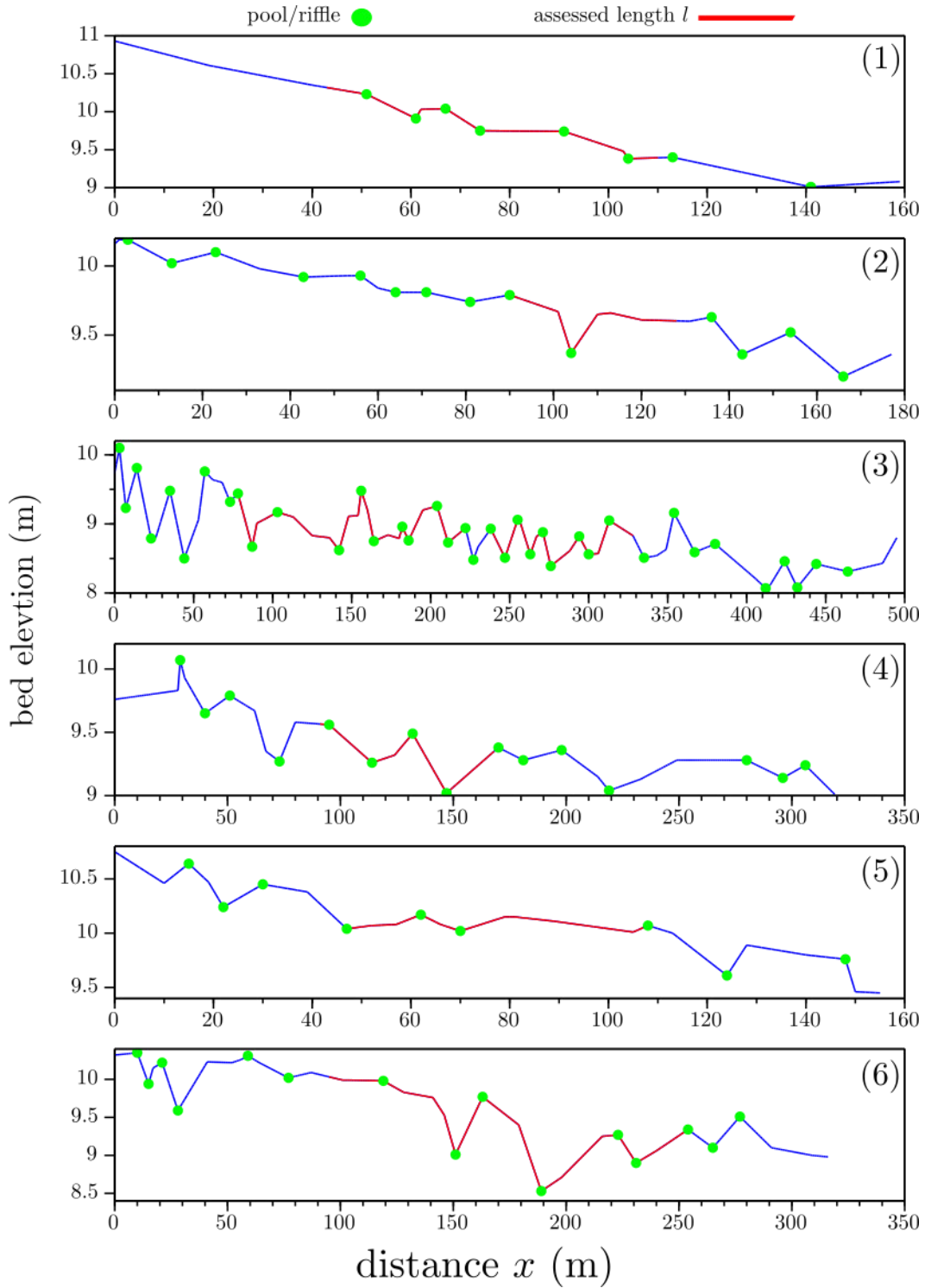
17 This was applied to all rivers and the results are depicted in the Fig. 10. Statistics of the BDT are shown in
18 Table 5 which displays a comparison between these two types of morphological units' identification and
19 mostly the identification of an average wavelength of the reach.

20 Fig. 10 shows the BDT results on all reaches, this method relies only on topography to determine the
21 positions of pools and riffles, moreover it also uses a threshold T (tolerance) but the technique does not need
22 a calibration reach or field investigation to know how to set this threshold. In this figure, Round points are
23 pools or riffles and from these points we can calculate the wavelengths and longitudinal spacing of each
24 reach as we stated before.

25 The work of the wavelet analysis is done on the assessed length l . However, the BDT method works on the
26 total length of the reaches. This was done to determine how effective the wavelength extracted by the
27 wavelet analysis can represent the entire reach even if an entire part is left unassessed.

28 For the wavelet method (Fig. 9), the wavelength extraction is among its objectives, while ~~for the BDT, the~~
29 ~~computation of the wavelength is done a sort of multiple calculations~~ does not directly calculate the
30 wavelength. It is computed by averaging the pool-to-pool and riffle-to-riffle distances. To compare these
31 two methods, we will use only the longitudinal spacing (λ^*) as a criterion.

32



1
 2 **Figure 10:** Results of the BDT method using a tolerance equal to the standard deviation on the total length and the
 3 assessed one (red) for all reaches (1 to 6). Round points are pools or riffles: pools are high and riffles are low points.
 4 In Table 5, we present results of the BDT on the total length L of all reaches and on the assessed length l .
 5 Using the total length L , the longitudinal spacings found with the BDT are close to the ones found with the
 6 wavelet analysis (deviation less than 1 time the bankfull width for the median), in all the reaches except the

1 Olivet (deviation of $4w_{bf}$). Over the assessed length ℓ we find very similar results with a deviations less
2 than one time the bankfull width. However, the shortening of the length ($\ell < L$) reduces the number of pools
3 and riffles identified (Graulade (1) and Avennelles (5)) and therefore introduces bias. This indicates that a
4 reasonable length greater than two cycles (pool-riffle) is always required to produce a pseudo-periodicity of
5 the reach by both methods, a condition which is clearly not fulfilled for all reaches of our dataset. But for
6 the other rivers except Olivet (3) and Orgeval (6) reaches, there is no much improvement if we replace the
7 total length with the assessed one. In this comparison, we found that the wavelengths extracted by the
8 multivariate wavelet analysis are generally included in the variance intervals of the wavelengths found by
9 the BDT. This was verified in all reaches except the Olivet River (3) where there is a big difference between
10 the longitudinal spacings found by BDT and by wavelets. This difference is due to the choice of the tolerance
11 value, which is low in our case to the point of not filtering out the high-frequency variability of bed elevation
12 and therefore gives a lower periodicity compared to the wavelets.

Reaches	1: Graulade	2: Semme	3: Olivet	4: Ozanne	5: Avennelles	6: Orgeval
Total length L (m)	160.0	177.0	495.0	319.0	155.0	318.0
Assessed length ℓ (m)	67.0	37.0	251.0	77.0	60.0	158.0
$\lambda_{Wav,mean}$ (m)	21.54	21.74	48.98	43.89	26.59	48.29
$\lambda_{BDT,mean}$ (m)	23.67	25.33	24.94	41.12	33.63	39.90
$\lambda_{\ell,BDT,mean}$ (m)	20.75	-	28.00	35.00	-	46.00
$\lambda^*_{Wav,mean}$	5.38	1.81	8.16	3.66	2.95	4.83
$\lambda^*_{BDT,mean}$	5.92	2.11	4.16	3.43	3.74	3.99
$\lambda^*_{\ell,BDT,mean}$	5.19	-	4.66	2.92	-	4.60
$\lambda_{Wav,median}$ (m)	21.55	21.84	51.70	43.49	26.54	48.78
$\lambda_{BDT,median}$ (m)	26.00	21.25	21.75	36.50	30.50	39.00
$\lambda_{\ell,BDT,median}$	20.75	-	23.50	35.00	-	46.00
$\lambda^*_{Wav,median}$	5.39	1.81	8.62	3.62	2.95	4.88
$\lambda^*_{BDT,median}$	6.5	1.77	3.63	3.04	3.39	3.90
$\lambda^*_{\ell,BDT,median}$	5.19	-	3.92	2.92	-	4.60
$\sigma(\lambda^*_{Wav,mean})$	0.09	0.07	0.70	0.08	0.04	0.34
$\sigma(\lambda^*_{BDT,mean})$	2.06	0.82	1.83	1.56	1.71	1.91
$\sigma(\lambda^*_{\ell,BDT,mean})$	2.21	-	2.30	-	-	0.71

13 **Table 5.** Results of BDT and the multivariate wavelet methods for all reaches. $\lambda_{meth,mean}$ is the mean wavelength
14 using one of the methods (for BDT, it used on total length and on the assessed one ℓ). $\lambda_{meth,median}$ is the median, and
15 $\lambda^*_{meth,mean}$ is the mean longitudinal spacing, $\lambda^*_{meth,median}$ is the median, and $\sigma(\lambda^*_{meth,mean})$ is the standard deviation
16 related to the longitudinal spacing. (-) means that we find only one longitudinal spacing which is the mean and the
17 median and there is no standard deviation.

18 5 – Discussion:

19 In this study, we consider the BDT method as a benchmark method. We do not consider a specific method
20 to be the “true” or “reference” one, we only apply these methods to have a general idea on the uncertainties
21 in the identification of morphological units. This method was chosen not because it is the ‘best’ method for
22 pool-riffle identification, but because it does not use thresholds (except for the tolerance T which does not
23 depend on field data). It means that it does not require a preliminary calibration of thresholds on velocity,
24 hydraulic radius, etc. on an independent reach (e.g., Wyrick and Pasternack, 2014 ; Hauer et al., 2009).
25 These thresholds vary from one reach to another and according to characteristics of each river. For this
26 reason, we didn’t compare our method with threshold methods on this dataset. In contrast, the results of the
27 longitudinal spacing intervals will be compared with literature.

1 For a long time, researchers have found common interval of longitudinal spacings that vary between 5 and
2 7 times the channel width (Leopold et al., 1964; Keller, 1972; Richards, 1976; Gregory et al., 1994). Keller
3 (1972) found that the median is less and varies between 3 and 5 the channel width. O’Neil and Abrahams
4 (1984), using BDT method, found the same results but with a median close to 3 the channel width and this
5 value can vary according to the tolerance T. Carling and Orr (2000) found lower values than before at about
6 3W. Recent studies (e.g., Wyrick and Pasternack, 2014) have calculated the longitudinal spacing of six
7 morphological units using 2D identification methods. The average of these pool and riffle spacings are,
8 respectively, 3.3 and 4.3 the channel width, which is less than the commonly accepted values of 5–7 W.

9 In this study, the longitudinal spacing vary in the mean and the median from ~1.8 to 8.6 times the bankfull
10 width, supporting the conclusion of Carling and Orr (2000) that pools are spaced approximately three to
11 seven times the channel width. However, the quoted longitudinal spacing relationships should be considered
12 in the context that the bankfull width and spacing distance are inherently variable even for short length
13 reaches. To illustrate this inherent variability, we found the example of Keller and Melhorn (1978) where
14 the pool-pool spacing values ranged from 1.5 to 23.3 channel widths, with an overall mean of 5.9 (Gregory
15 et al., 1994; Knighton, 2014). This variability in longitudinal spacing is probably related to a short assessed
16 length, a small number of cross-sections surveyed, or other factors such as geology, bank characteristics
17 (cohesion), grain size of the river bed, artificial channel modifications, etc.

18 We worked with a dataset that contains cross-sections spaced 0.46 to 2.9 times bankfull width. Other studies
19 have used much shorter spacings (e.g., Pasternack et al., 2018b; Legleiter, 2014b) to identify morphological
20 units. Of course, the larger the number of cross-sections, the more robust the identified correlations will be.
21 In addition, we worked with irregularly spaced cross-sections, which will normally lead to biases in the
22 results. Despite this, the "biased" placement does not impairs the overall methodology. This methodology
23 has provided good results in terms of longitudinal spacings and therefore it can be applied for a shorter
24 cross-section spacings to clearly identify these alternate morphologies. The short lengths we found raise
25 questions about the naturality of the rivers. In our case, the rivers are subject to artificial modifications (e.g.,
26 bridges, weirs) and rehabilitations, which will have a significant impact on the hydro-morphological
27 parameters (width, depth, meandering, etc.). This can have a very important impact on the identification of
28 pseudo-periods.

29 The wavelet ridge analysis is powerful in identifying pseudo-periods, amplitude and phase while respecting
30 the correlations between parameters. We can thus identify alternating morphological units in a more
31 objective way in terms of frequency/wavenumber.

32 This wavelength can be used to represent the variability of the bathymetry in hydraulic models in cases
33 where we do not have a full access to the geometry of the channel (e.g., remote sensing data as the
34 overcoming Surface Water and Ocean Topography Mission) and the morphology can be modelled by
35 pseudo-periodic functions. Furthermore, it can be implemented in synthetic geometry generators (e.g., River
36 Builder, Pasternack and Zhang. (2020)) where the bathymetry and sinuosity wavelengths extracted by the
37 wavelets can be used to model meandering rivers with alternating morphologies. Ultimately, hydraulic
38 modeling will be the true test of the potential of a pseudo-periodic equivalent geometry (e.g. for simulating
39 a reach-average rating curve).-From this extracted common wavelength using the flow parameters, it is
40 possible to represent the topography continuously.

41 On the other hand, it represents drawbacks compared to other methods. First, the cone of influence that
42 ignores a large part of the river and sometimes biases the results (in the case of the Graulade (1) and Semme
43 (2) reaches) in the case of small total lengths. ~~It is the region of the wavelet spectrum in which edge effects~~
44 ~~become important. We can say the same thing~~ Similarly for reach length and number of morphological units

1 as for the number of cross-sections: the larger it is, the more robust the results will be, and the smaller the
2 relative portion of “unassessed length” will be. Still, the method remains a powerful tool for non-stationary
3 analysis. Another problem is the amplitude which is sometimes overestimated in some regions of the
4 topography. We visualized this in several cases in our study, since we used the Neperian logarithm to avoid
5 negative values and therefore the inverse function (exponential) will give slightly larger values. However,
6 this does not bias the identified wavelength of the reach.

7 **6 – Conclusions:**

8 In this study, we present an automatic procedure based on Wavelet Ridge extraction to identify some
9 characteristics of alternating morphological units (MU), such as their longitudinal spacing and amplitude.
10 The method does not rely on any a priori thresholds to identify MU sequences. It was applied to six rivers
11 with a maximum length of 500 meters. We chose to work with classical hydro-morphological variables
12 (velocity, hydraulic radius, bed shear stress) in addition to the local channel direction angle that evaluates
13 the impact of river sinuosity in the determination of the wavelength.

14 ~~On the overall~~ As a result, identified wavelength are consistent with values of the literature (mean in 3-7
15 w_{bf}). The use of a multivariate approach yields more robust results than the univariate approaches, by
16 ensuring a consistent covariance of flow variables in the pseudo-periodic behavior.

17 Given the short length of several reaches, the relatively small number of cross-sections for each reach, and
18 the possible impacts of artificial modifications, this paper is mainly a proof-of-concept of the wavelet
19 approach. It does not preclude the long-term possibility of extending the work to other rivers with other
20 types of MUs, other longer reaches with a large number of cross-sections.

21
22 Acknowledgements: The authors acknowledge financial support from the French National Space Agency
23 (Centre National d’Etudes Spatiales, CNES) and Sorbonne University through the Ph.D. grant of M.
24 Mahdade. We would also like to thank G.B. Pasternack, the second anonymous reviewer, and the editor for
25 the valuable suggestions and comments that greatly helped improve this paper.

26 **Appendix A: List of symbols**

$A_{i,mod}$:	Signal amplitude of the shape of the modeled variable number i
$A(x)$:	Cross-section area
A_m :	Signal amplitude of the shape
$\cos(\theta)$:	Cosine of local channel direction angle
$\cos(\theta)_{mod}$:	Modeled cosine of local channel direction angle
f :	Space series function
f_i :	Measured space series function number i
$f_{i,mod}$:	Modeled space series function number i with multivariate wavelet analysis
f_{mod} :	Modeled variable with the univariate wavelet analysis
g :	Acceleration due to gravity and its value is 9.81 m.s^{-2}
J :	Energy slope (m.m^{-1})
$k(x)$:	Wavenumber (rad.m^{-1})
$K(x)$:	Local wavenumber that corresponds to the maximum variance of the signal (rad.m^{-1})
<u>$K_i(x)$:</u>	<u>Local wavenumber that corresponds to the maximum variance of the variable i (rad.m^{-1})</u>
ℓ :	$K(x)$ support (m)
L :	Total reach length (m)
N :	Number of total chosen variables

n	Manning's roughness coefficient
$P(x)$	Wetted perimeter
Q_{\min} :	Minimum discharge modeled ($m^3.s^{-1}$)
$R(x,s)$ or $R(x,k)$ or R	Absolute value or modulus of the wavelet transform at a position x and with a scale s or wavenumber k
R_h	Hydraulic radius (m)
$R_{h,mod}$	Modeled hydraulic radius (m)
s :	Dilation or scale factor
S :	Reach slope ($m.m^{-1}$)
S_D	Standard deviation of the bed elevation difference series (m)
T :	Tolerance value, which is the minimum absolute value of the cumulative elevation change required for the identification of pools and riffles (m)
$v(x)$	Velocity ($m.s^{-1}$)
v_{mod}	Modeled velocity ($m.s^{-1}$)
v_{obs}	Mesured velocity ($m.s^{-1}$)
$w(x)$:	Reach width in the x abscissa (m)
w_{bf} :	Reach bankfull width (m)
w_m	Mean width (m)
x :	Translation factor in the wavelet transform or the abscissa position (m)
$y = y_{\max}$:	Water depth measured from the the talweg elevation $y = z_{ws} - z$ (m)
y_m :	Mean depth (m)
z or $z_{t,Obs}$:	Measured bed elevation or talweg elevation (m)
$z_{t,Uni}$:	Modeled bed elevation using the univariate wavelet analysis (m)
$z_{t,Multi}$:	Modeled bed elevation using the Multivariate wavelet analysis (m)
z_{ws} :	Water surface elevation measured from the ONGF (m)
α :	Fourier factor associated with the wavelet ($m.rad^{-1}$)
β :	Dimensionless frequency taken to be 6 recommended by Torrence and Compo (1998)
λ :	Reach wavelength (m)
λ^* :	Typical pool (riffle) spacing or dimensionless reach wavelength or longitudinal spacing
ρ :	Water density ($997kg/m^3$)
$\sigma(w)$:	Standard deviation of the width along the reach (m)
$\sigma()$:	Standard deviation
$\tau_b(x)$:	Bed shear stress in the x abscissa (Pa)
$\tau_{b,mod}(x)$:	Modeled bed shear stress in the x abscissa (Pa)
$\theta(x)$:	local channel direction angle which is the local angular deviation of the channel direction from a lower-frequency curve (degrees)
Φ :	Corresponding phase at the position x and the wavenumber K with $\Phi(x) = \phi(x, K(x))$ (rad)
Φ_i :	Phase at the position x and the wavenumber K for the variable number i
$\phi(x, s)$ or $\phi(x, k)$ or ϕ :	Phase or argument at a position x and with a scale s or wavenumber k (rad)
ϕ_i :	Phase of the variable number i
ψ :	Mother wavelet function
$\psi_{s,x}$:	Daughter wavelet function
η :	Dimensionless position parameter
\mathbb{C} :	Complex numbers
\mathbb{R} :	<u>Real numbers</u>
\mathbb{R}_+ :	<u>Positive real numbers</u>
$W[f](x,s)$:	Continuous wavelet transform of $f(x)$ with the wavelet ψ

1

2 Appendix B: Mathematical calculus for the wavelet transform

3 1 – The univariate case

4 The conjugate form of the mother wavelet is:

$$\psi^*(\eta) = \pi^{-\frac{1}{4}} e^{-i\beta\eta - \frac{\eta^2}{2}} \quad (\text{B1})$$

5 Its derivative in relation to the mute variable η is:

$$\begin{aligned} \psi^{*'}(\eta) &= -\pi^{-\frac{1}{4}} (i\beta + \eta) e^{-i\beta\eta - \frac{\eta^2}{2}} \\ &= -(i\beta + \eta) \psi^*(\eta) \end{aligned} \quad (\text{B2})$$

6 In section 3 - 1, η is a mute integration variable and x appears only in the argument $\alpha k(\xi - x)$ of the
7 function ψ^* . By applying the derivation formula of a composite function, the derivative of the wavelet
8 transform is expressed by:

$$\begin{aligned} \frac{\partial}{\partial x} W[f(x)](x, k) &= \sqrt{\alpha k} \int_{-\infty}^{+\infty} f(\eta) \frac{\partial}{\partial x} [\psi^*(\alpha k(\eta - x))] d\eta \\ &= \sqrt{\alpha k} \int_{-\infty}^{+\infty} f(\eta) (-\alpha k) \psi^{*'}(\alpha k(\eta - x)) d\eta \\ &= (\alpha k) \sqrt{\alpha k} \int_{-\infty}^{+\infty} f(\eta) (i\beta + \alpha k(\eta - x)) \psi^*(\alpha k(\eta - x)) d\eta \\ &= (\alpha k) \sqrt{\alpha k} \int_{-\infty}^{+\infty} [(i\beta - \alpha k x) f(\eta) + \alpha k \eta f(\eta)] \psi^*(\alpha k(\eta - x)) d\eta \\ &= (\alpha k) (i\beta - \alpha k x) W[f(x)](x, k) + (\alpha k)^2 W[x f(x)](x, k) \end{aligned} \quad (\text{B3})$$

9 On the other hand, we have:

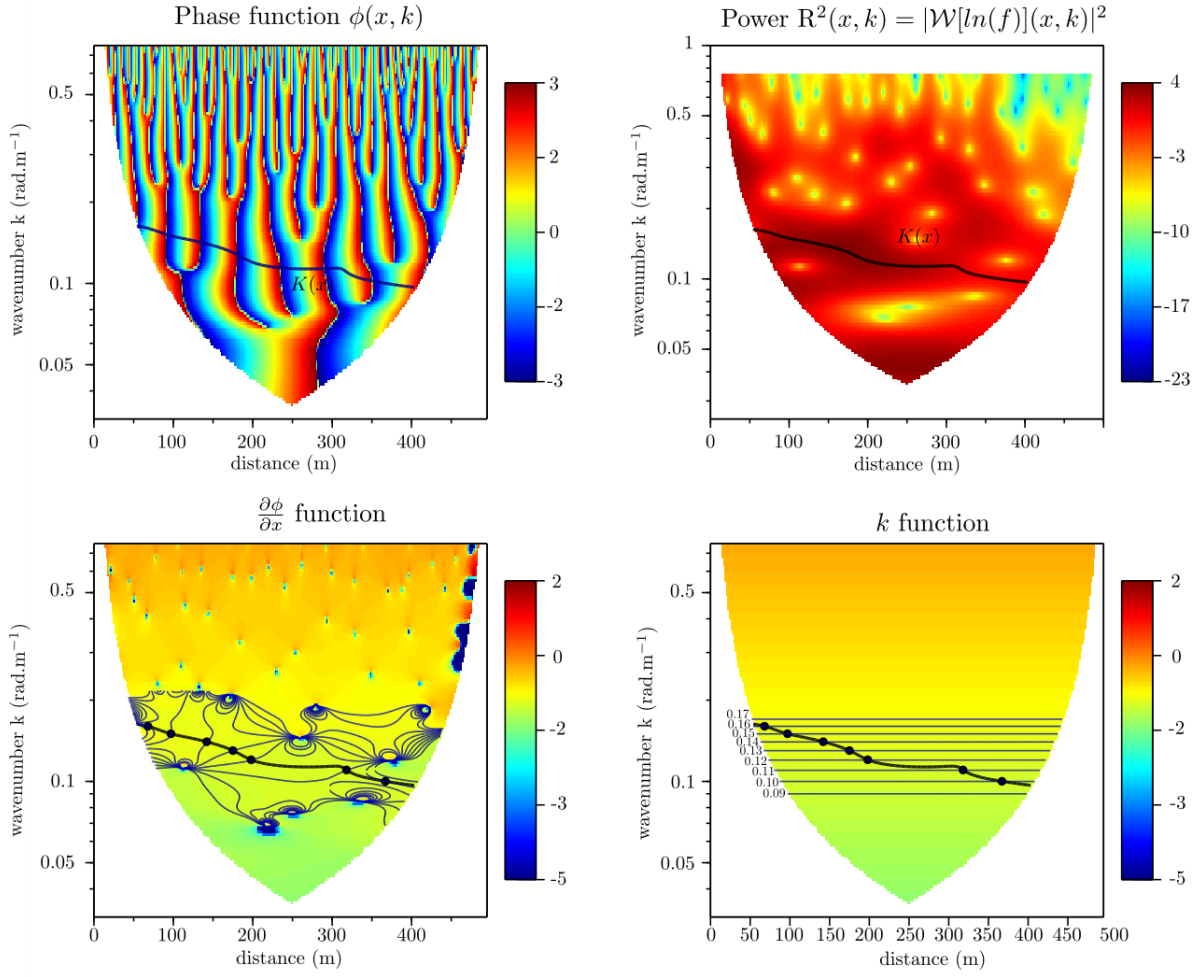
$$\begin{aligned} \frac{\partial}{\partial x} W[f(x)](x, k) &= \frac{\partial}{\partial x} (R(x, k) e^{i\phi(x, k)}) \\ &= \left[\frac{1}{R(x, k)} \frac{\partial R(x, k)}{\partial x} + i \frac{\partial \phi(x, k)}{\partial x} \right] R(x, k) e^{i\phi(x, k)} \end{aligned} \quad (\text{B4})$$

$$\begin{aligned} \frac{\partial}{\partial x} \text{Re}(\ln W[f(x)](x, k)) &= \frac{1}{R(x, k)} \frac{\partial R(x, k)}{\partial x} = \text{Re} \left(\frac{1}{W[f(x)](x, k)} \frac{\partial}{\partial x} W[f(x)](x, k) \right) \\ \frac{\partial}{\partial x} \text{Im}(\ln W[f(x)](x, k)) &= \frac{\partial \phi(x, k)}{\partial x} = \text{Im} \left(\frac{1}{W[f(x)](x, k)} \frac{\partial}{\partial x} W[f(x)](x, k) \right) \end{aligned} \quad (\text{B5})$$

10 Finally:

$$\begin{aligned} \frac{\partial \phi(x, k)}{\partial x} &= \text{Im} \left((\alpha k) (i\beta - \alpha k x) + (\alpha k)^2 \frac{W[x f(x)](x, k)}{W[f(x)](x, k)} \right) \\ \frac{\partial \phi(x, k)}{\partial x} &= (\alpha k) \beta + (\alpha k)^2 \text{Im} \left(\frac{W[x f(x)](x, k)}{W[f(x)](x, k)} \right) \end{aligned} \quad (\text{B6})$$

11 The previous expression numerically avoids the derivative of the function $\phi(x, k)$, which varies quickly for
12 large wavenumbers.



1
2 **Figure B1.** Steps of determining the local wavenumber $K(x)$ using the wavelet univariate ridge analysis of the the
3 velocity of the Olivet (3) reach, represented in the four panels. (A) The phase function $\phi(x, k)$; (B) the power's cone
4 of influence of the wavelet to characterize the region where there is a maximum variability of the velocity in Neperian
5 logarithm; (C) the function $\frac{\partial \phi(x, k)}{\partial x}$; (D) the function k .

6 2 – The multivariate case

7 In the multivariate case, we should resolve the Eq. 20 which contain three derivatives to compute. The first
8 one is already done in the univariate case which is:

$$\frac{\partial \phi_i(x, k)}{\partial x} = (\alpha k) \beta + (\alpha k)^2 \text{Im} \left(\frac{W[xf_i(x)]}{W[f_i(x)]} \right) \quad (\text{B7})$$

9 The second one is the computation of $\frac{\partial^2 \phi_i(x, k)}{\partial k \partial x}$:

$$\frac{\partial^2 \phi_i(x, k)}{\partial k \partial x} = \alpha \beta + 2\alpha^2 k \text{Im} \left(\frac{W[xf_i(x)]}{W[f_i(x)]} \right) + (\alpha k)^2 \text{Im} \left(\frac{\partial}{\partial k} \left(\frac{W[xf_i(x)]}{W[f_i(x)]} \right) \right) \quad (\text{B8})$$

10 For that we should develop $\frac{\partial}{\partial k} \left(\frac{W[xf_i(x)]}{W[f_i(x)]} \right)$:

$$1 \quad \frac{\partial}{\partial k} \left(\frac{W[xf_i(x)]}{W[f_i(x)]} \right) = \frac{1}{W[f_i(x)]} \frac{\partial W[xf_i(x)]}{\partial k} - \frac{W[xf_i(x)]}{(W[f_i(x)])^2} \frac{\partial W[f_i(x)]}{\partial k}$$

2 We calculate each derivative:

$$3 \quad \frac{\partial W[f_i(x)]}{\partial k} = \left(\frac{1}{\sqrt{k}} \frac{\partial \sqrt{k}}{\partial k} \right) W[f_i(x)] + \sqrt{\alpha k} \int_{-\infty}^{+\infty} f(\eta) \frac{\partial}{\partial k} [\psi^*(\alpha k(\eta - x))] d\eta$$

$$4 \quad = \left(\frac{1}{2k} \right) W[f_i(x)] + \sqrt{\alpha k} \int_{-\infty}^{+\infty} f(\eta) \alpha(\eta - x) \psi^{*'}(\alpha k(\eta - x)) d\eta$$

$$5 \quad = \left(\frac{1}{2k} \right) W[f_i(x)] + \sqrt{\alpha k} \int_{-\infty}^{+\infty} f(\eta) \alpha(\eta - x) (i\beta + \alpha k(\eta - x)) \psi^*(\alpha k(\eta - x)) d\eta$$

$$6 \quad = \left(\frac{1}{2k} \right) W[f_i(x)] + \sqrt{\alpha k} \int_{-\infty}^{+\infty} [(i\beta - \alpha^2 k x^2) + (-i\beta\alpha + 2\alpha^2 k x)\eta - (\alpha^2 k)\eta^2] f(\eta) \psi^*(\alpha k(\eta - x)) d\eta$$

$$7 \quad = \left(\frac{1}{2k} - \alpha^2 k x^2 + i\beta\alpha x \right) W[f_i(x)] + (2\alpha^2 k x - i\beta\alpha) W[xf_i(x)] - (\alpha^2 k) W[x^2 f_i(x)]$$

8 We find a general formulation with $p=0 \dots N$:

$$9 \quad \frac{\partial W[x^p f_i(x)]}{\partial k} = \left(\frac{1}{2k} - \alpha^2 k x^2 + i\beta\alpha x \right) W[x^p f_i(x)] + (2\alpha^2 k x - i\beta\alpha) W[x^{p+1} f_i(x)]$$

$$10 \quad - (\alpha^2 k) W[x^{p+2} f_i(x)]$$

11 The third one is the computation of $\frac{\partial^3 \phi_i(x, k)}{\partial k^2 \partial x}$:

$$\frac{\partial^3 \phi_i(x, k)}{\partial k^2 \partial x} = 2\alpha^2 \text{Im} \left(\frac{W[xf_i(x)]}{W[f_i(x)]} \right) + 4\alpha^2 k \text{Im} \left(\frac{\partial}{\partial k} \left(\frac{W[xf_i(x)]}{W[f_i(x)]} \right) \right)$$

$$+ (\alpha k)^2 \text{Im} \left(\frac{\partial^2}{\partial k^2} \left(\frac{W[xf_i(x)]}{W[f_i(x)]} \right) \right) \quad (\text{B9})$$

12

$$13 \quad \frac{\partial^3 \phi_i(x, k)}{\partial k^2 \partial x} = 2\alpha^2 \text{Im} \left(\frac{W[xf_i(x)]}{W[f_i(x)]} \right) + 4\alpha^2 k \text{Im} \left(\frac{\partial}{\partial k} \left(\frac{W[xf_i(x)]}{W[f_i(x)]} \right) \right) + (\alpha k)^2 \text{Im} \left(\frac{\partial^2}{\partial k^2} \left(\frac{W[xf_i(x)]}{W[f_i(x)]} \right) \right)$$

14 With :

$$15 \quad \frac{\partial^2}{\partial k^2} \left(\frac{W[xf_i(x)]}{W[f_i(x)]} \right) = \frac{1}{W[f_i(x)]} \frac{\partial^2 W[xf_i(x)]}{\partial k^2} - \frac{W[xf_i(x)]}{(W[f_i(x)])^2} \frac{\partial^2 W[f_i(x)]}{\partial k^2} - \frac{2}{(W[f_i(x)])^2} \frac{\partial W[f_i(x)]}{\partial k} \frac{\partial W[xf_i(x)]}{\partial k}$$

16

- 1
- 2 Alfieri, L., Feyen, L., Salamon, P., Thielen, J., Bianchi, A., Dottori, F., and Burek, P.: Modelling the socio-
3 economic impact of river floods in Europe, *Natural Hazards and Earth System Sciences*, 16, 1401–1411,
4 2016.
- 5 Baume, J.-P. and Poirson, M.: Modélisation numérique d'un écoulement permanent dans un réseau
6 hydraulique maillé à surface libre, en régime fluvial, *La houille blanche*, pp. 95–100, 1984.
- 7 Box, G. E. and Jenkins, G. M.: *Time series analysis: Forecasting and control* San Francisco, Calif: Holden-
8 Day, 1976.
- 9 Brown, R. A. and Pasternack, G. B.: Bed and width oscillations form coherent patterns in a partially
10 confined, regulated gravel-cobble-bedded river adjusting to anthropogenic disturbances, *Earth Surface*
11 *Dynamics*, 5, 1, 2017.
- 12 Brown, R. A., Pasternack, G. B., and Wallender, W. W.: Synthetic river valleys: Creating prescribed
13 topography for form–process inquiry and river rehabilitation design, *Geomorphology*, 214, 40–55, 2014.
- 14 Carling, P. A. and Orr, H. G.: Morphology of riffle-pool sequences in the River Severn, England, *Earth*
15 *Surface Processes and Landforms*, 25, 369–384, 2000.
- 16 Carmona, R. A., Hwang, W. L., and Torrèsani, B.: Multiridge detection and time-frequency reconstruction,
17 *IEEE transactions on signal processing*, 47, 480–492, 1999.
- 18 Clifford, N. J.: Formation of riffle—pool sequences: field evidence for an autogenetic process, *Sedimentary*
19 *Geology*, 85, 39–51, 1993.
- 20 Dury, G.: Osage-type underfitness on the River Severn near Shrewsbury, Shropshire, England, *Background*
21 *to palaeohydrology*, Wiley, Chichester, 399, 1983.
- 22 [Frothingham, K. M., & Brown, N. \(2002\). Objective identification of pools and riffles in a human-modified](#)
23 [stream system. *Middle States Geographer*, 35, 52-60.](#)
- 24 Gabor, D.: Theory of communication. Part 1: The analysis of information, *Journal of the Institution of*
25 *Electrical Engineers-Part III: Radio and Communication Engineering*, 93, 429–441, 1946.
- 26 Gangodagamage, C., Barnes, E., and Fofoula-Georgiou, E.: Scaling in river corridor widths depicts
27 organization in valley morphology, *Geomorphology*, 91, 198–215, 2007.
- 28 Gregory, K., Gurnell, A., Hill, C., and Tooth, S.: Stability of the pool-riffle sequence in changing river
29 channels, *River Research and Applications*, 9, 35–43, 1994.
- 30 Grimaldi, S., Li, Y., Walker, J., and Pauwels, V.: Effective Representation of River Geometry in Hydraulic
31 Flood Forecast Models, *Water Resources Research*, 54, <https://doi.org/10.1002/2017WR021765>, 2018.
- 32 Grinsted, A., Moore, J. C., and Jevrejeva, S.: Application of the cross wavelet transform and wavelet
33 coherence to geophysical time series, *Nonlinear processes in geophysics*, 11, 561–566, 2004.
- 34 Harvey, A.: Some aspects of the relations between channel characteristics and riffle spacing in meandering
35 streams, *American Journal of Science*, 275, 470–478, 1975.

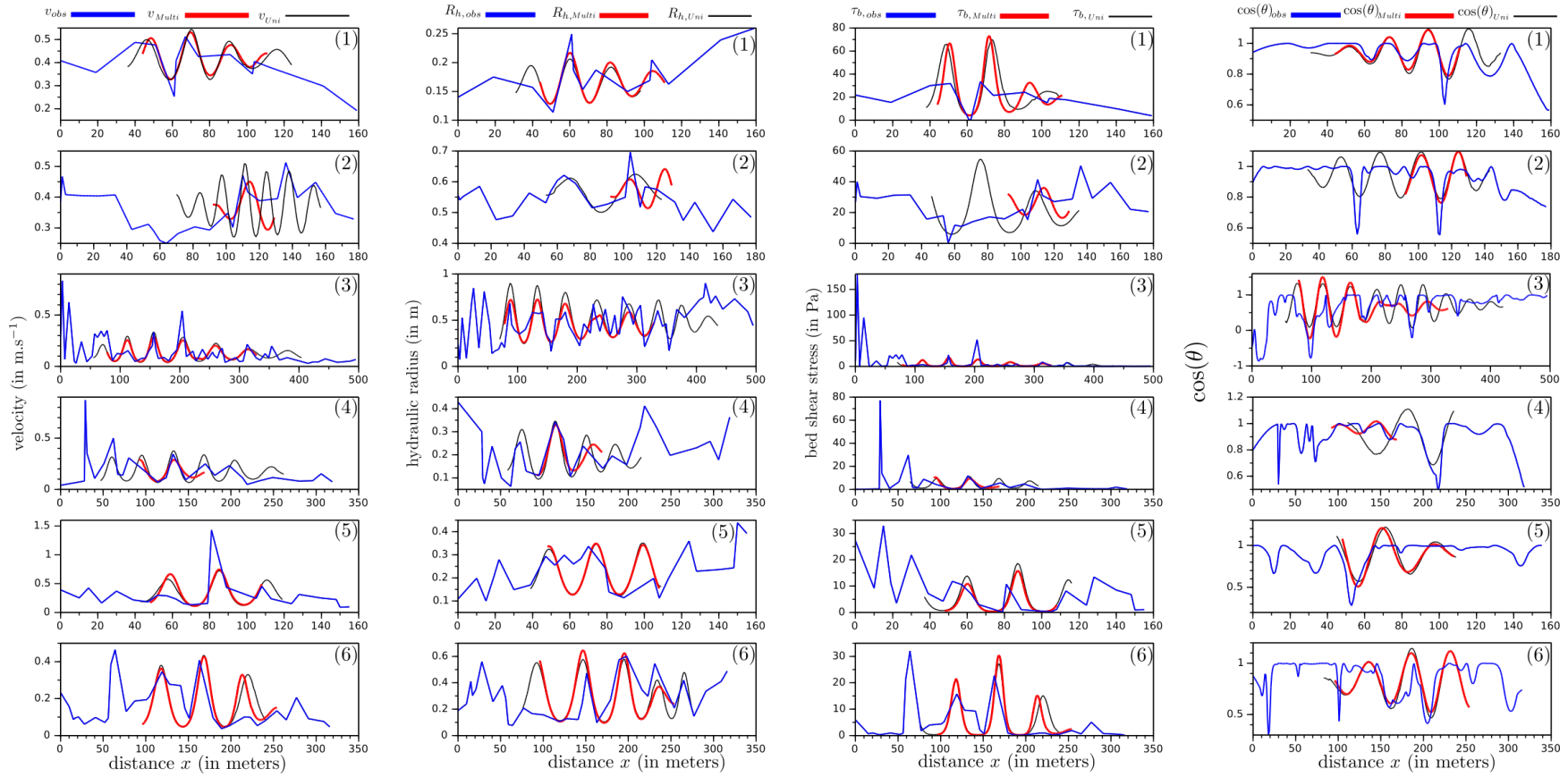
- 1 Hauer, C., Mandlbürger, G., and Habersack, H.: Hydraulically related hydro-morphological units:
2 description based on a new conceptual mesohabitat evaluation model (MEM) using LiDAR data as
3 geometric input, *River Research and Applications*, 25, 29–47, 2009.
- 4 Hauer, C., Unfer, G., Tritthart, M., Formann, E., and Habersack, H.: Variability of mesohabitat
5 characteristics in riffle-pool reaches: Testing an integrative evaluation concept (FGC) for MEM-application,
6 *River research and applications*, 27, 403–430, 2011.
- 7 Higuchi, H., Lewalle, J., and Crane, P.: On the structure of a two-dimensional wake behind a pair of flat
8 plates, *Physics of Fluids*, 6, 297–305, 1994.
- 9 Hogan, D. L. et al.: Channel morphology of unlogged, logged, and debris torrented streams in the Queen
10 Charlotte Islands, Ministry of Forests and Lands, 33 1986.
- 11 Jowett, I. G.: A method for objectively identifying pool, run, and riffle habitats from physical measurements,
12 *New Zealand journal of marine and freshwater research*, 27, 241–248, 1993.
- 13 Katul, G. G. and Parlange, M. B.: Analysis of land surface heat fluxes using the orthonormal wavelet
14 approach, *Water Resources Research*, 31, 2743–2749, 1995a.
- 15 Katul, G. G. and Parlange, M. B.: The spatial structure of turbulence at production wavenumbers using
16 orthonormal wavelets, *Boundary-Layer Meteorology*, 75, 81–108, 1995b.
- 17 Katul, G. G., Parlange, M. B., and Chu, C. R.: Intermittency, local isotropy, and non-Gaussian statistics in
18 atmospheric surface layer turbulence, *Physics of Fluids*, 6, 2480–2492, 1994.
- 19 Keller, E.: Development of alluvial stream channels: a five-stage model, *Geological Society of America*
20 *Bulletin*, 83, 1531–1536, 1972.
- 21 Keller, E. and Melhorn, W.: Bedforms and fluvial processes in alluvial stream channels: selected
22 observations, *Fluvial geomorphology*, pp. 253–283, 1973.
- 23 Keller, E. and Melhorn, W.: Rhythmic spacing and origin of pools and riffles, *Geological Society of*
24 *America Bulletin*, 89, 723–730, 1978.
- 25 Knighton, A.: Asymmetry of river channel cross-sections: Part I. Quantitative indices, *Earth Surface*
26 *Processes and Landforms*, 6, 581–588, 1981.
- 27 Knighton, D.: *Fluvial forms and processes*: London, Edward Arnold, 1998.
- 28 Knighton, D.: *Fluvial forms and processes: a new perspective*, Routledge, 2014.
- 29 Kondolf, G. M.: Geomorphological stream channel classification in aquatic habitat restoration: uses and
30 limitations, *Aquatic Conservation: Marine and Freshwater Ecosystems*, 5, 127–141, 1995.
- 31 Krueger, A. and Frothingham, K.: Application and comparison of geomorphological and hydrological pool
32 and riffle quantification methods, *Geogr Bull*, 48, 85–95, 2007.
- 33 Kumar, P.: Role of coherent structures in the stochastic-dynamic variability of precipitation, *Journal of*
34 *Geophysical Research: Atmospheres*, 101, 26 393–26 404, 1996.
- 35 Kumar, P. and Foufoula-Georgiou, E.: A multicomponent decomposition of spatial rainfall fields: 1.
36 Segregation of large-and small-scale features using wavelet transforms, *Water Resources Research*, 29,
37 2515–2532, 1993.

- 1 Lashermes, B. and Foufoula-Georgiou, E.: Area and width functions of river networks: New results on
2 multifractal properties, *Water Resources Research*, 43, 2007.
- 3 Legleiter, C. J.: A geostatistical framework for quantifying the reach-scale spatial structure of river
4 morphology: 1. Variogram models, related metrics, and relation to channel form, *Geomorphology*, 205, 65–
5 84, 2014a.
- 6 Legleiter, C. J.: A geostatistical framework for quantifying the reach-scale spatial structure of river
7 morphology: 2. Application to restored and natural channels, *Geomorphology*, 205, 85–101, 2014b.
- 8 Leopold, L., Wolman, M., and Miller, J.: *Fluvial processes in geomorphology*, Freeman, San Francisco,
9 1964.
- 10 Lilly, J. M. and Olhede, S. C.: Higher-order properties of analytic wavelets, *IEEE Transactions on Signal*
11 *Processing*, 57, 146–160, 2008.
- 12 Lilly, J. M. and Olhede, S. C.: On the analytic wavelet transform, *IEEE Transactions on Information Theory*,
13 56, 4135–4156, 2010.
- 14 Lilly, J. M. and Olhede, S. C.: Analysis of modulated multivariate oscillations, *IEEE Transactions on Signal*
15 *Processing*, 60, 600–612, 2011.
- 16 Mallat, S.: *A wavelet tour of signal processing*, Elsevier, 1999.
- 17 McKean, J., Nagel, D., Tonina, D., Bailey, P., Wright, C. W., Bohn, C., and Nayegandhi, A.: Remote
18 sensing of channels and riparian zones with a narrow-beam aquatic-terrestrial LIDAR, *Remote Sensing*, 1,
19 1065–1096, 2009.
- 20 Milne, J.: Bed-material size and the riffle-pool sequence, *Sedimentology*, 29, 267–278, 1982.
- 21 Milne, J. and Sear, D.: Modelling river channel topography using GIS, *International Journal of Geographical*
22 *Information Science*, 11, 499–519, 1997.
- 23 Montgomery, D. R., Buffington, J. M., Smith, R. D., Schmidt, K. M., and Pess, G.: Pool spacing in forest
24 channels, *Water Resources Research*, 31, 1097–1105, 1995.
- 25 Muzy, J.-F., Bacry, S. E., and Arneodo, A.: Multifractal formalism for fractal signals: The structure-function
26 approach versus the wavelet transform modulus-maxima method, *Physical review E*, 47, 875, 1993.
- 27 Navratil, O.: Débit de pleins bords et géométrie hydraulique: une description synthétique de la morphologie
28 des cours d'eau pour relier le bassin versant et les habitats aquatiques, 2005.
- 29 Navratil, O., Albert, M., Herouin, E., and Gresillon, J.: Determination of bankfull discharge magnitude and
30 frequency: comparison of methods on 16 gravel-bed river reaches, *Earth Surface Processes and Landforms*,
31 31, 1345–1363, 2006.
- 32 Neal, J. C., Odoni, N. A., Trigg, M. A., Freer, J. E., Garcia-Pintado, J., Mason, D. C., Wood, M., and Bates,
33 P. D.: Efficient incorporation of channel cross-section geometry uncertainty into regional and global scale
34 flood inundation models, *Journal of Hydrology*, 529, 169–183,
- 35 Ng, E. K. and Chan, J. C.: Geophysical applications of partial wavelet coherence and multiple wavelet
36 coherence, *Journal of Atmospheric and Oceanic Technology*, 29, 1845–1853, 2012.
- 37 Nordin, C. F.: *Statistical properties of dune profiles*, vol. 562, US Government Printing Office, 1971.

- 1 Nourani, V., Baghanam, A. H., Adamowski, J., and Kisi, O.: Applications of hybrid wavelet–Artificial
2 Intelligence models in hydrology: A review, *Journal of Hydrology*, 514, 358–377, 2014.
- 3 O’Neill, M. P. and Abrahams, A. D.: Objective identification of pools and riffles, *Water resources research*,
4 20, 921–926, 1984.
- 5 Ozkurt, N. and Savaci, F. A.: Determination of wavelet ridges of nonstationary signals by singular value
6 decomposition, *IEEE Transactions on Circuits and Systems II: Express Briefs*, 52, 480–485, 2005.
- 7 Pasternack, G. and Arroyo, R.: *RiverBuilder: River Generation for Given Data Sets*, R package version 0.1,
8 2018.
- 9 Pasternack, G. B. and Brown, R. A.: 20 Ecohydraulic Design of Riffle-Pool Relief and Morphological Unit
10 Geometry in Support of Regulated Gravel-Bed River Rehabilitation, in: *Ecohydraulics*, p. 337, Wiley
11 Online Library, 2013.
- 12 Pasternack, G. B. and Hinnov, L. A.: Hydrometeorological controls on water level in a vegetated
13 Chesapeake Bay tidal freshwater delta, *Estuarine, Coastal and Shelf Science*, 58, 367–387, 2003.
- 14 Pasternack, G.B. and Zhang, M. 2020. River Builder User’s Manual For Version 1.0.0. University of
15 California, Davis, CA. <https://github.com/RiverBuilder/RiverBuilder>
- 16 Richards, K.: The morphology of riffle-pool sequences, *Earth Surface Processes and Landforms*, 1, 71–88,
17 1976a.
- 18 Richards, K.: Channel width and the riffle-pool sequence, *Geological Society of America Bulletin*, 87, 883–
19 890, 1976b.
- 20 Rodríguez, J. F., García, C. M., and García, M. H.: Three-dimensional flow in centered pool-riffle
21 sequences, *Water Resources Research*, 49, 30 202–215, 2013.
- 22 Rosgen, D. L.: The cross-vane, w-weir and j-hook vane structures... their description, design and application
23 for stream stabilization and river restoration, in: *Wetlands engineering & river restoration 2001*, pp. 1–22,
24 2001.
- 25 Rossi, A., Massei, N., and Laignel, B.: A synthesis of the time-scale variability of commonly used climate
26 indices using continuous wavelet transform, *Global and Planetary Change*, 78, 1–13, 2011.
- 27 Saleh, F., Ducharme, A., Flipo, N., Oudin, L., and Ledoux, E.: Impact of river bed morphology on discharge
28 and water levels simulated by a 1D Saint–Venant hydraulic model at regional scale, *Journal of hydrology*,
29 476, 169–177, 2013.
- 30 Schaefli, B., Maraun, D., and Holschneider, M.: What drives high flow events in the Swiss Alps? Recent
31 developments in wavelet spectral analysis and their application to hydrology, *Advances in Water Resources*,
32 30, 2511–2525, 2007.
- 33 Schneider, K. and Vasilyev, O. V.: Wavelet methods in computational fluid dynamics, *Annual Review of*
34 *Fluid Mechanics*, 42, 473–503, 2010.
- 35 Schweizer, S., Borsuk, M. E., Jowett, I., and Reichert, P.: Predicting joint frequency distributions of depth
36 and velocity for instream habitat assessment, *River Research and Applications*, 23, 287–302, 2007.
- 37 Thompson, D. M.: 5 Random controls on semi-rhythmic spacing of pools and riffles in constriction-
38 dominated rivers, *Earth Surface Processes and Landforms*, 26, 1195–1212, 2001.

- 1 Thomson, D. J.: Spectrum estimation and harmonic analysis, *Proceedings of the IEEE*, 70, 1055–1096,
2 1982.
- 3 Torrence, C. and Compo, G. P.: A practical guide to wavelet analysis, *Bulletin of the American*
4 *Meteorological society*, 79, 61–78, 1998.
- 5 Trigg, M. A., Wilson, M. D., Bates, P. D., Horritt, M. S., Alsdorf, D. E., Forsberg, B. R., and Vega, M. C.:
6 Amazon flood wave hydraulics, *Journal of Hydrology*, 374, 92–105, 2009.
- 7 Wadeson, R.: A geomorphological approach to the identification and classification of instream flow
8 environments, *Southern African Journal of Aquatic Science*, 20, 38–61, 1994.
- 9 Wheaton, J. M., Pasternack, G. B., and Merz, J. E.: Spawning habitat rehabilitation-I. Conceptual approach
10 and methods, *International Journal of River Basin Management*, 2, 3–20, 2004.
- 11 Wyrick, J. and Pasternack, G.: Geospatial organization of fluvial landforms in a gravel–cobble river: beyond
12 the riffle–pool couplet, *Geomorphology*, 213, 48–65, 2014.
- 13 Wyrick, J. R., Senter, A. E., and Pasternack, G. B.: Revealing the natural complexity of fluvial morphology
14 through 2D hydrodynamic delineation of river landforms, *Geomorphology*, 210, 14–22, 2014.
- 15 Yang, C. T.: Formation of Riffles and Pools, *Water Resources Research*, 7, 1567–1574,
16 <https://doi.org/10.1029/WR007i006p01567>, <http://dx.doi.org/10.1029/WR007i006p01567>, 1971.

1 Supplementary materials:



2
3 **Figure S1:** Comparison between the univariate and the multivariate results for the six reaches (from 1 to 6) and using the four variables (velocity, hydraulic radius,
4 bed shear stress, and cosine of local channel direction angle)